

Stochastic Framework for Inverse Consistent Registration

by

YEUNG, Sai Kit

A Thesis Submitted to
The Hong Kong University of Science and Technology
in Partial Fulfillment of the Requirements for
the Degree of Master of Philosophy
in Bioengineering

Copyright © by Yeung, Sai Kit (2005)
ALL RIGHTS RESERVED.

June 2005, Hong Kong

Authorization

I hereby declare that I am the sole author of the thesis.

I authorize the Hong Kong University of Science and Technology to lend this thesis to other institutions or individuals for the purpose of scholarly research.

I further authorize the Hong Kong University of Science and Technology to reproduce the thesis by photocopying or by other means, in total or in part, at the request of other institutions or individuals for the purpose of scholarly research.

YEUNG, Sai Kit

Stochastic Framework for Inverse Consistent Registration

by

YEUNG, Sai Kit

This is to certify that I have examined the above MPhil thesis
and have found that it is complete and satisfactory in all respects,
and that any and all revisions required by
the thesis examination committee have been made.

Professor Pengcheng SHI, Thesis Supervisor

Professor Oscar C.L. AU, Thesis Examination Chairperson

Professor Chi-Keung TANG, Thesis Examination Examiner

Prof. I-Ming Hsing, Program Director

Bioengineering Graduate Program, School of Engineering
10 June 2005

Acknowledgements

This thesis would not have been possible without the support of many people.

Many thanks to my supervisor, Professor Pengcheng Shi, who read my numerous revisions. His positive teaching attitude and immense knowledge benefit many ways in my life.

Thanks to Professor Oscar Au, chairperson of my thesis examination committee who carefully examine my work. His patience and advice is appreciated.

I would like to thank Professor Chi-Keung Tang, who has given guidance and encouragement to me throughout my undergraduate and postgraduate studies.

Also thanks to my colleagues of the Medical Image Computing Group, including Huafeng Liu, Xin Yuan, Wai Bun Lo, Lung Ngong Wong, Chun Lok Wong, Hon Pong Ho, Shan Tong, and Heye Zhang, who offered me guidance, patience and support.

Thanks to my parents and my sister, for their love, support and encouragement ever since I was born. They are the most wonderful people in the world. Without them, this thesis would not have been possible.

And finally, thanks to all my friends. The pleasure they gave me supplied me energy to continue my work even during the harshest moments.

Contents

Title Page	i
Authorization Page	ii
Signature Page	iii
Acknowledgements	iv
Contents	v
List of Figures	vii
List of Tables	xi
Abstract	xii
1 Introduction	1
1.1 Background	1
1.2 Contributions	2
1.3 Structure of the Thesis	3
2 Review of Related Works	4
2.1 Introduction	4
2.2 Inverse Consistency through incorporation of sub-objective cost function	5
2.3 Deterministic Inverse Consistency Representation	6
3 Inverse Consistency in Registration	7

3.1	Introduction	7
3.2	Registration of Continuous Signals	8
3.3	Discrete Nature of the Information Sources	10
3.4	Role of Inverse Consistency in Registration	13
4	Stochastic Inverse Consistency	16
4.1	Introduction	16
4.2	Stochastic Inverse Consistent Representation	17
4.3	GTLS Formulation	18
4.4	Inverse Consistency by Iterative GTLS Solution	22
5	Experiments and Discussions	25
5.1	Introduction	25
5.2	Experiments on Synthetic Image Data	25
5.2.1	Data Description	26
5.2.2	Results and Discussions	26
5.3	Experiments on Point Sets Data	27
5.3.1	Data Description	28
5.3.2	Results and Discussions	29
5.4	Experiments on Real Image Data	32
5.4.1	Data Description	32
5.4.2	Results and Discussions	32
5.5	Convergency Issue	33
6	Conclusion	50
6.1	Summary	50
6.2	Future Work	51

List of Figures

3.1	Registration of (a): A and B , (b): A_c and B_c . (c),(d): The matching criteria curves for forward and backward registration process. (e),(f): The combined matching criteria curve (NMIC) from the forward and reverse registration process.	9
3.2	(a),(b): Registration of A_c and B_c . (c),(d): The matching criteria curves for forward and backward registration process. (e),(f): The combined matching criteria curve (NMIC) from the forward and reverse registration process.	10
3.3	Left side: Forward registration process. Right side: Backward registration process. Row 1: Input pair. Point correspondences during: Row 2: 1st iteration, Row 3: 70th iteration, Row 4: last iteration	12
3.4	(a): forward registration result T_{12} (blue circles) with the inverse of backward registration result T_{21}^{-1} (purple triangles), (b): backward registration result T_{21} (blue circles) with the inverse of forward registration result T_{12}^{-1} (purple triangles). The transformations involved are affine.	13
5.1	(a): Image A. (b): Image B. (c): Image C: Image B downsampled by 2 in x and y dimensions.	26
5.2	(a)-(c): transformations represented the forward warping results, left to right: $T_{12}, T_{12}^*, T_{21}^{-1}$. (d)-(f): transformations represented the backward warping results, left to right: $T_{12}^{-1}, T_{21}^*, T_{21}$. The red contours are the warped boundary of the object in image A for row 1 and image B for row 2 with the warping by the transformations specified above.	27

5.3	(a)-(c): transformations represented the forward warping results, left to right: $T_{12}, T_{12}^*, T_{21}^{-1}$. (d)-(f): transformations represented the backward warping results, left to right: $T_{12}^{-1}, T_{21}^*, T_{21}$. The red contours are the warped boundary of the object in image A for row 1 and image C for row 2 with the warping by the transformations specified above.	28
5.4	Registering black crosses to black circles. Left column and right column represent the forward and backward registration process respectively. The red or blue triangles above are the warping results from the transformations specified below the corresponding figures.	29
5.5	(a) and (b) are the results for the forward and backward point matching processes respectively. The red and blue triangles and the green stars are the warping results of the black crosses by the transformations specified in the corresponding figures.	30
5.6	(a): Brain image with the extracted point sets. (b): Testing point sets (blue circles) with the reference point sets (black crosses).	31
5.7	(a) and (b) are the visual results for the forward and backward point matching processes respectively. The red and blue triangles and the green stars are the warping results of the black crosses by the transformations specified in the corresponding figures. (c) and (d) are the plots of the sum of squared distances (SSD) for input point sets with different standard deviation of gaussian noise.	35
5.8	(a): Brain image with the extracted point sets. (b): Testing point sets (blue circles) with the reference point sets (black crosses).	36
5.9	(a) and (b) are the visual results for the forward and backward point matching processes respectively. The red and blue triangles and the green stars are the warping results of the black crosses by the transformations specified in the corresponding figures. (c) and (d) are the plots of the sum of squared distances (SSD) for input point sets with different standard deviation of gaussian noise.	37
5.10	Brain image with the representing point set.	38

5.11	Column 1 and 2 are examples of small deformation and large deformation respectively. (a),(b) are the point set without any noise and outliers. In (c), positions of the points are perturbed by gaussian noise with standard deviation = 2. In (d), outliers are added to the reference point set.	39
5.12	Column 1 and 2 are the results for registering reference point sets with small and large deformation respectively. (a) shows forward registration results for small deformation with outlier proportion = 0.1. (b) shows the backward registration results for large deformation with gaussian noise of S.D = 4 added. (c)-(f) are the plots of the sum of squared distances (SSD) for input point sets with different standard deviation of gaussian noise. While (c),(d) are for the forward registration process, (e),(f) are for the backward one.	40
5.13	Column 1 and 2 are the results for registering reference point sets with small and large deformation respectively. (a)-(d) are the plots of the sum of squared distances (SSD) for input point sets with different proportion of outliers added. While (c),(d) are for the forward registration process, (e),(f) are for the backward one.	41
5.14	Column 1 and 2 are the results for registering reference point sets with small and large deformation respectively. (a)-(d) are the plots of the consistency error, measured by $\ T_{12} * T_{21} - I \ _F$ for the input transformation pair and $\ T_{12}^* * T_{21}^* - I \ _F$ for the GTLS output. While (c) and (d) are plots under different S.D of gaussian noise, (e) and (f) are plots for different proportion of outliers added.	42
5.15	Registering pair I_1 and I_2	43
5.16	Registration results for the forward and backward registration process are shown in column 1 and column 2 respectively.	44
5.17	The registration results for the forward and backward registration process are shown in (a) and (b) respectively.	45

5.18	Convergency Profile (CP) example for experiments of brain point sets: (a): Small deformation + noise. (b): Large deformation + noise. (c): Small deformation + outliers. (d): Large deformation + outliers. The noise in (a) and (b) is gaussian noise with zero mean, S.D = 4. Outlier proportion = 0.4 in (c) and (d).	45
5.19	The mean value (Mean CP), together with the maximum value (Max CP), minimum value (Min CP) and +/- 1 S.D. from the mean value (Mean CP+1SD/Mean CP-1SD) of the convergency profile from the studies of different amounts of noise or outliers. (a): Small deformation + noise. (b): Large deformation + noise. (c): Small deformation + outliers. (d): Large deformation + outliers. The number of studies in each case is 5.	46
5.20	Zoom in of Fig.5.19	47
5.21	Percentage change of the convergency error shown in the convergency profiles in Fig.5.18. (a): Small deformation + noise. (b): Large de- formation + noise. (c): Small deformation + outliers. (d): Large deformation + outliers.	48
5.22	(a): An example of convergency profile which can not converge monoton- ically. (b): The percentage change of the convergency profile.	48
5.23	Input to the GTLS system which cause the problematic convergency in Fig.5.22. (a): The purple triangles are transformed from the blue circles by transformation matrix T_{12} . (b): The purple triangles are transformed from the blue circles by transformation matrix T_{21} . T_{12} and T_{21} is the transformation matrices pair for our system input. . . .	49

List of Tables

5.1	Sum of squared distances (SSD) from different transformations results.	30
-----	------------------------------------------------------------------------	----

Registration

by YEUNG, Sai Kit

Bioengineering

Department of Chemical Engineering

The Hong Kong University of Science and Technology

ABSTRACT

Registration is the process of extracting spatial correspondences between different data sets such as digital images or sets of points and obtaining their spatial transformations from the extracted spatial correspondences. The information provided by these transformations is very useful in areas such as morphing in computer graphics, fusion of medical images from different modalities, and finding the pose of an object in an image or between different objects.

One of the essential criteria in registration is inverse consistency, i.e. to make the registration source-destination symmetric so that the forward and backward mapping matrices extracted are inverse to each other. Conventional approaches enforce consistency in deterministic fashions, either through the incorporation of sub-objective cost function that impose consistent property during the registration process or by the construction of diffeomorphic mapping on predetermined landmarks sets. However, deterministic techniques for establishing the consistency means that the errors inherited from the discrete nature of the information sources are not considered. In this thesis, we present a stochastic framework that yields perfect inverse consistent registration from the initial forward and backward matching matrices. These initial forward and backward transformation matrices can be computed by any image registration or point matching algorithms, which are input to our system. Then an optimization process is developed to compute the perfect source-destination symmetric mapping between the forward and backward transformation matrices. The errors

of the registration matrices and the imperfectness of the consistent constraint are both modelled such that the whole optimization process is stochastic in nature. An iterative generalized total least square (GTLS) strategy has been developed such that the source-destination symmetric criterion is optimally established. Experiments based on point sets matching where ground truths are available, and synthetic as well as real image registration problems have been performed. Both show very promising results.

Chapter 1

Introduction

1.1 Background

Registration is a useful technique in computer vision and image analysis. It aims at extracting the spatial correspondences between different data sets. Then by these established spatial correspondences, the corresponding data sets can be aligned or transformed to one another so that it is easier to relate their corresponding features. The data sets involved in the registration process can be different unstructured point sets, landmarks or digital images. Registration problem on point sets is usually referred to point matching problem while image registration is the registration process applied among different images.

The information obtained from the registration process is very useful in many aspects. The correspondences extracted can be used as the basis for morphing between different objects [34]. The transformations derived can transform images to a computer model or align different features in an image that have different locations in physical space. Relating corresponding features is particularly important in medical image analysis. With the advancements of noninvasive imaging technologies, medical images are increasing in health care and in biomedical research. Different imaging modalities emphasize different structures, for example, X ray Computed Tomography (CT) images show bone structures while Magnetic Resonance (MR) images can reveal tissues properties. Registration makes the integration of information from different

modalities possible and it has been one of the hot topics in medical image analysis [12], [29], [19].

One of the most desirable properties for registration is inverse consistency or source-destination symmetry in which the correspondence is one-to-one and also unambiguous. Consistent transformations maintain the topology of the registering pair. This is important in medical imaging for generating biologically meaningful results [9] and in computer vision 3D points are usually re-projected onto the image to see if they match with the original pixel color [17], however, this property is usually not ensured during the registration process. Most of the earlier registration efforts do not attempt to impose consistency while deriving the transformation matrices, such as the landmark or point based methods [3, 4, 11, 22], the contours based algorithm [26, 25], the surface-based algorithms [20, 27], and the volume based methods which utilize the whole image information [2, 37, 10, 18, 32].

More recently, consistency has received increasing attention in point set and image registration. The inverse consistent constraint has been imposed along with other information such as image intensity and geometric characteristics to become part of the optimization criterion in medical image registration [9] and to act as subjective cost function to ensure coupling in point set matching [14]. Since the source-destination symmetry is only part of the metric that needs to be minimized, the resulting transformation matrices are, in general, not perfectly consistent. Further, the transformations are solved in deterministic nature, meaning that the stochastic error properties of these matrices are not considered.

1.2 Contributions

We propose a stochastic framework for point set and image registration which results in perfect source-destination symmetric mapping between the data sets. Instead of imposing inverse consistency in a *deterministic* and *imperfect* sense, we enforce the inverse consistent property optimally with the systematic considerations of stochastic uncertainties of the input forward and backward transformation matrices to achieve

perfect source-destination symmetry. The adoption of the Generalized Total Least Square (GTLS) technique [31] allows for simultaneous considerations of the errors in the input transformation matrices and the inverse consistent constraint during a post-registration fitting process. A set of new forward and backward transformations are solved iteratively until they are *perfectly inverse* to each other. We want to point out that the contribution of this thesis is *not* in presenting a new registration algorithm per se, but rather a novel way for imposing the stochastic inverse consistent constraint given an estimated set of registration matrices. This framework can be used with any registration algorithms which have already shown their validity in establishing forward/backward mappings for different matching problems. Experimental results on point set matching, synthetic and real image registration demonstrate the superior performance of the proposed method.

1.3 Structure of the Thesis

This thesis is organized as follows:

In chapter 2, different registration algorithms that yield the inverse consistent property for different types of registration problems are reviewed.

In chapter 3, the inherited error of the registration process due to discrete nature of information sources is illustrated. Then the role of inverse consistency in registration is discussed in depth. Apart from this, we also discuss how inverse consistency generates better registration results from the forward and backward registration processes.

Chapter 4 examines the methodologies used in detail. In this chapter, our stochastic inverse consistent model for inverse consistent registration is presented, where the iterative generalized total least square (GTLS) approach is described to show how the source-destination symmetric transformations pair is optimally obtained.

In chapter 5, experimental results of different point sets, synthetic images and real medical images are shown and compared with the conventional methods. The study about convergency issue is presented in the last of this chapter. Chapter 6 concludes this thesis and suggests different possible future research directions.

Chapter 2

Review of Related Works

2.1 Introduction

Conventional registration methods usually do not consider the consistency constraint. Due to different reasons such as the discrete nature of information sources and the local optimization process in the registration algorithms, the transformations extracted from the forward and backward registration processes are always ambiguous. It means given two images or two sets of points I_1 and I_2 . The result of registering I_1 to I_2 will not be an exact inverse of the result from registering I_2 to I_1 .

In many situations, the registration process is only performed in one of the direction, i.e., we are only registering I_1 to I_2 or I_2 to I_1 to establish the spatial correspondences between the two data sets. In that sense, we are missing the information from one of the directions. Moreover, if we do not enforce the inverse consistent constraint, even we have the registration results from both direction, it would be difficult to combine or choose the result between them.

One would argue that we can perform the registration process in one of the direction, then we take the inverse of that transformation result to obtain a source-destination symmetric pair. However, in real situation, the registering data is not simple and the ground truth is not available. The images and point sets are so complicated that it is very difficult to tell whether the result from the forward or backward registration process is better without the ground truth evaluation. As a result, simply

taking one of the registration results may bear the risk of choosing the worse result. So inverse consistency indeed provides a mean to utilize the information from both direction and provide a more robust registration result.

In recent years, different methods are proposed to enforce source-destination symmetric in registration. A common approach is imposing the inverse consistent constraint during the registration process through incorporation of sub-objective cost function, then the optimization of the matching criteria will include the inverse consistent constraint. For all of these approaches, there is an implicit assumption that the transformation matrices extracted from the matching criteria at the global maximum is the ground truth. That means they are both deterministic in nature that inherent error associated with the matching criteria is not considered in these approaches.

2.2 Inverse Consistency through incorporation of sub-objective cost function

A common strategy for enforcing consistency is the incorporation of sub-objective cost function in the matching criteria. Different works that incorporate consistency under various conditions and matching criteria have been proposed Christensen etal [9, 16, 8, 15, 7]. Their scheme for incorporating consistent constraint in registration is to assign a cost metric E_{Cons} to the consistent property as part of the matching cost function E , i.e.,

$$E = E_{Sim} + E_{Cons} \tag{2.1}$$

where E_{Sim} measures the similarity (i.e. image intensity and geometrical properties) between the data sets. Since the consistent measure is only part of the overall cost function, the optimal solution to Equ.(2.1) in general would not produce the perfect inverse consistent mapping one desires. The diffeomorphic point matching in [14] follows similar pattern, where the cost function is combined with different sub-objective functions including the diffeomorphic measurement.

2.3 Deterministic Inverse Consistency Representation

The above formulations do not consider the underlying stochastic properties associated with the transformation results solved from the matching criteria. It means throughout the registration process, the matching criteria is absolutely trusted so that the forward transformation T_{12} and the backward transformation T_{21} are solved in *deterministic* nature in order to get a one-to-one consistent mapping (unambiguous correspondence), i.e.,

$$T_{12} * T_{21} = I \tag{2.2}$$

In the following chapters, we will examine the possible drawbacks of simply imposing the deterministic model for inverse consistency. We will also show that due to the discrete nature of information sources, even the optimization process utilizes a global strategy, the results produced are still not equal to the ground truth. In other words, the matching criteria cannot be trusted fully and there will always be uncertainties associated with the transformation matrices obtained.

The role of inverse consistent constraint will also be discussed. In reported literatures, inverse consistency is usually discussed as the property being imposed on the registration so that the registration process can maintain certain kind of topology. Actually inverse consistency is the art of how to integrate the information from the forward and backward registration processes. A proper combination between the two can yield a better registration result than results using only forward or only backward registration. This observation will be discussed in next chapter.

Chapter 3

Inverse Consistency in Registration

3.1 Introduction

In this chapter, we illustrate the main problems due to the discrete nature of the information sources in registration process and the role of inverse consistency in registration. The discrete nature of the digital images or a set of points makes the registration problems ill-posed. This is because the registering signals are actually unable to represent the real continuous signals perfectly. As a result, the optimum by any matching criteria is only the best match for a pair of discrete signals, instead of the real continuous signals. Registration results obtained therefore will always contain errors and not equal the ground truth.

Apart from the discrete nature of information sources, the optimization process is also discrete. This is another problem since the discrete optimization process will always result in ambiguous forward and backward transformation pair if it is a local optimization. So in order to guarantee a source-destination symmetric transformation pair, we have to optimize the forward and backward registration processes simultaneously. Here, we explain the role of inverse consistent constraint and how it enforces the simultaneous optimization between the two registration processes. How inverse consistency results in better registration results is usually not mentioned in other literatures [9], [13], [28]. In the last section, we will illustrate the potential of an inverse consistent registration that improves the registration results towards the ground

truth.

3.2 Registration of Continuous Signals

First, it should be noted that it is always valid to have a deterministic consistent constraint if we are registering continuous objects. Fig.3.1(a) are 2 continuous sine curves A and B , $A = \sin(x)$ and $B = \sin(x-0.5)$ such that B is shifted to right by 0.5s from A . The matching criteria we use to demonstrate the registration profile for these two signals is the Normalized Mutual Information (NMI) [24] which has its maximum when two signals are perfectly aligned as shown in Fig.3.1(c). Here we refer registering B to A as the forward registration process and registering A to B as the backward registration process. It is easy to observe that there are two distinct optima for the corresponding ground truth transformation in the forward and backward registration process. They are -0.5 in the matching criteria curve for the forward registration process (NMIf) and +0.5 in the matching criteria curve for the backward registration process (NMIr). So it means that the matching criteria can result in ground truth transformation in the registration process, i.e., the forward and backward transformation matrices resolved should be perfectly representing their true spatial relationship. In addition, the results solved from the forward and backward registration processes will be a perfect inverse of each others. In this situation, the consistent property between the solved forward and backward transformations is automatically established. As a result, if we are registering a pair of continuous objects, imposing consistent constraint or not during the registration process will not have any effect and the registration result is in indeed the ground truth transformation. The inverse of this registration result will immediately become its forward/backward counterpart transformation result.

Therefore if there is a digital signal that is sampled under very high sampling rate such that the original continuous signal can be perfectly reconstructed, the deterministic model for inverse consistency can always be imposed. In Fig.3.1(b), the registering pair A_c and B_c reconstruct the original signal A and B perfectly, making

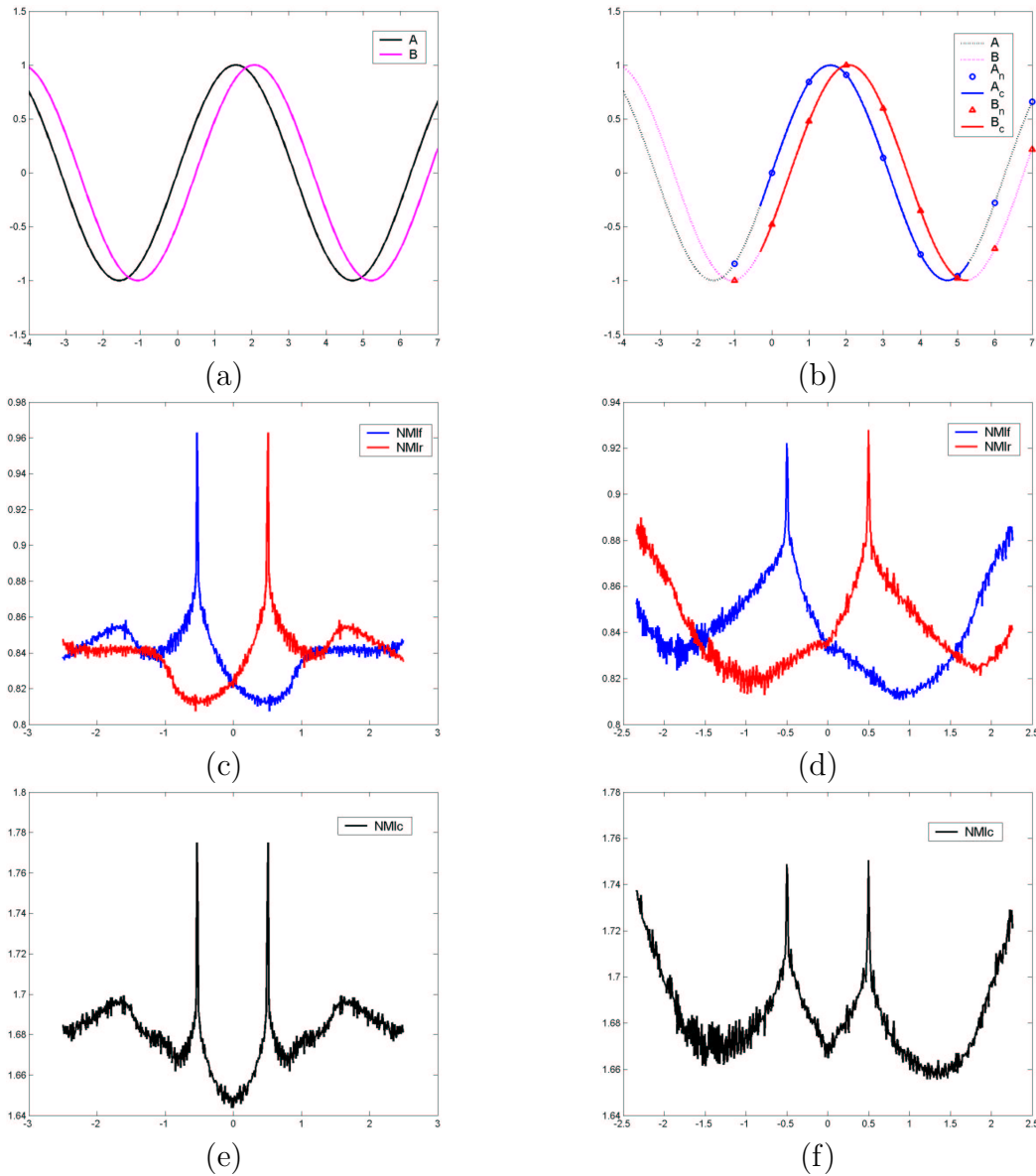


Figure 3.1: Registration of (a): A and B , (b): A_c and B_c . (c),(d): The matching criteria curves for forward and backward registration process. (e),(f): The combined matching criteria curve (NMIC) from the forward and reverse registration process.

the forward and reverse registration processes result in the ground truth and achieve source-destination symmetry (Fig.3.1(d)). Such a case would be registration for two images under very high resolution, e.g CT-CT registration in medical image registration problem.

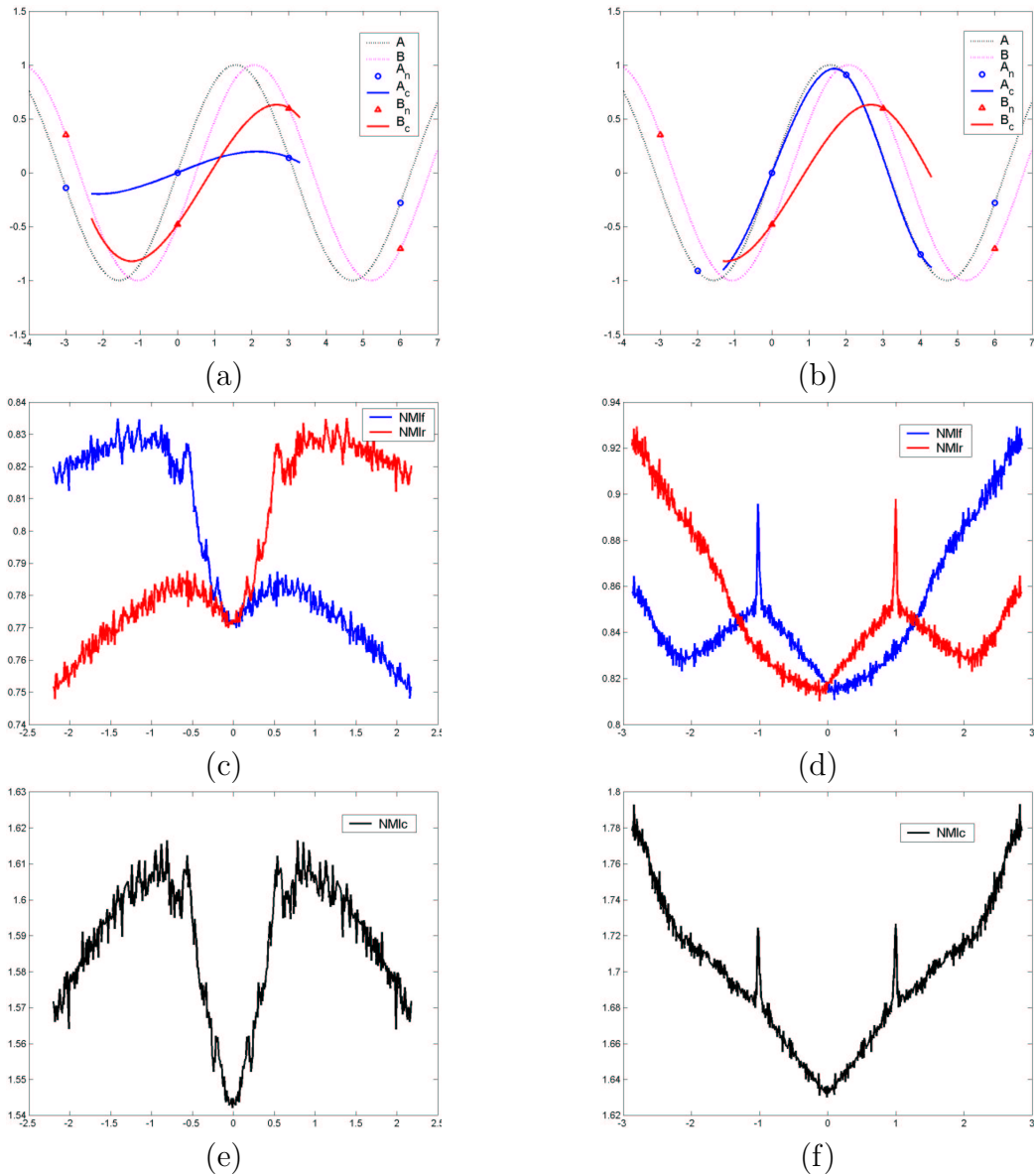


Figure 3.2: (a),(b): Registration of A_c and B_c . (c),(d): The matching criteria curves for forward and backward registration process. (e),(f): The combined matching criteria curve (NMlc) from the forward and reverse registration process.

3.3 Discrete Nature of the Information Sources

In the previous section we have shown that if we are registering continuous objects, or the digitized objects can fully reconstruct the original continuous objects, the source-destination symmetric constraint will be unnecessary since performing one of the forward or backward registration process and then simply inverting the result produces a pair of ground truth transformations. However, since the digital images or the discrete point sets we used are not able to perfectly represent the original objects, the above situation is no longer valid. This is the key problem from the discrete nature

of the information sources because this means that the registering pair we pass to the registration algorithms is actually different from the original signals. One can easily see that the resulting transformation will not be perfectly equal to the ground truth transformation which will be illustrated in the following examples.

Fig.3.2(a) is the first example to illustrate the idea. A_n and B_n are the digitized version of A and B both with sampling interval of $3s$. Although their corresponding sampling rate is still above the Nyquist frequency ($\frac{1}{\pi}$ for $\sin(x)$), it is shown that the reconstructed signals A_c and B_c are unable to represent the original signals perfectly. As a result, the matching criteria are no longer able to give you the ground truth transformations. The maxima are now around $(-1.1, 1.1)$ instead of the sharp peaks at $(-0.5, 0.5)$ in the forward and backward matching materia curves (Fig.3.2(c)). Fig.3.2(b) is another example with A_n at a higher sampling rate ($2s$). Fig.3.2(d) shows the maxima for the forward and backward registration process which would be -1 and 1 respectively instead of -0.5 and 0.5 . In both cases, even global optimization algorithms are used, the results obtained are not correct.

In the above situation, the source-destination symmetric property may still be obtained without enforcing inverse consistent constraint if the forward and backward registration process can reach their corresponding global optimum by global optimization algorithm. However, in most case the registration algorithms utilize local optimization algorithm to extract the transformations. This will be problematic for the case when a distinguish global optimum is not available, so that trapping in local optimum is more likely to occur and the extracted transformations are further away from the ground truth. This problem may be avoided if a very sharp optimum is available. In Fig.3.2(d), the two peaks are outstanding and it can be expected that even local optimization process is carried on the two curves separately, the results obtained will still be inverse consistent, i.e., $-1, 1$. But this situation is not guaranteed especially in high dimension. Moreover, in conventional registration problems, the optimization process is usually initialized in the same starting direction, i.e., we just initialize one way to start climbing the hill (the matching criteria curve), e.g. climbing the hill from left to right. From Fig.3.2(c), the possible forward and backward registration results

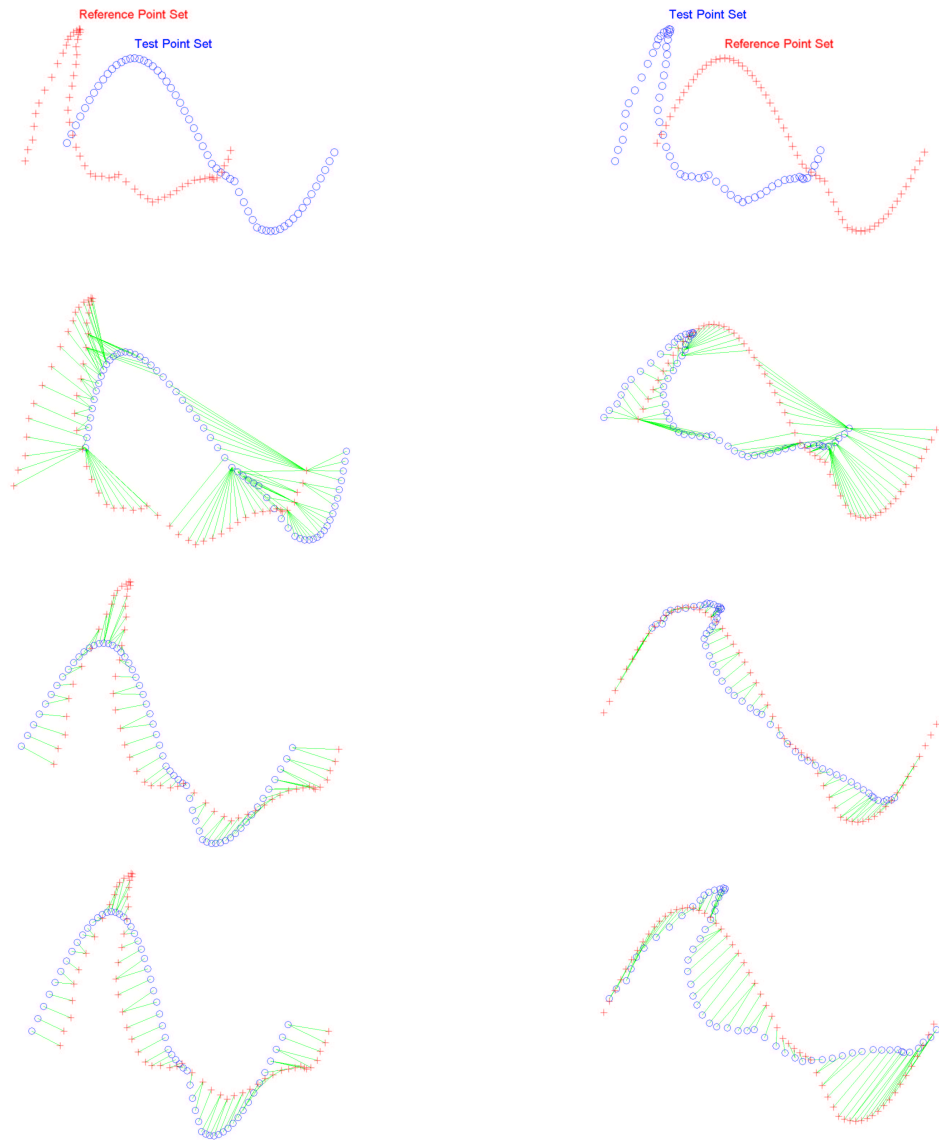


Figure 3.3: Left side: Forward registration process. Right side: Backward registration process. Row 1: Input pair. Point correspondences during: Row 2: 1st iteration, Row 3: 70th iteration, Row 4: last iteration

would be $(-1.1, -0.5)$ instead of the ground truth pair $(-0.5, 0.5)$ means that there are both error in the transformation results and they are also ambiguous.

Another problem occurs when the ambiguous transformation pair is an inconsistent correspondence established during the registration process. This problem is very common in typical point matching process since the point correspondences established from the forward and backward point matching processes are always going to be different. The intermediate correspondences of the forward and backward process are ambiguous so that the final transformations obtained are inconsistent. This situation

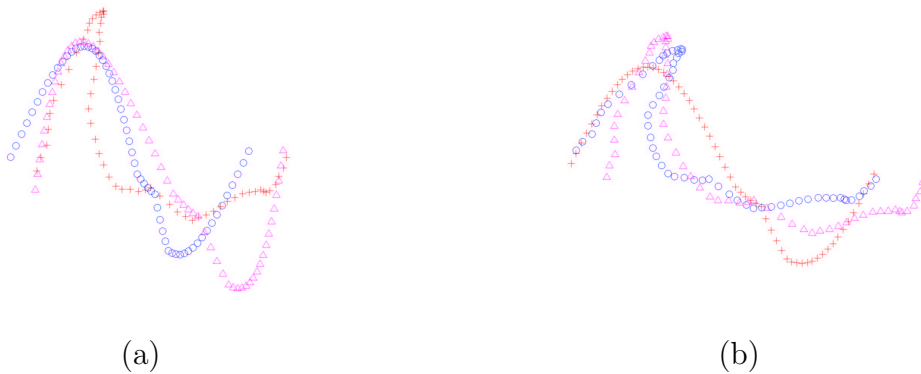


Figure 3.4: (a): forward registration result T_{12} (blue circles) with the inverse of backward registration result T_{21}^{-1} (purple triangles), (b): backward registration result T_{21} (blue circles) with the inverse of forward registration result T_{12}^{-1} (purple triangles). The transformations involved are affine.

is illustrated in Fig.3.3. We simply swap the input for the point matching algorithm (in our case ICP [3]), the correspondences pairs during the iteration are linked by green lines in Fig.3.3(b)-(d). In Fig.3.4, the final forward and backward transformations and their corresponding inverses are used on the original testing point set to warp on the reference point set to show the two transformations are not source-destination symmetric.

From the above examples, we can conclude that due to the discrete nature of the information sources, the optimum in the matching criteria cannot represent the real ground truth in continuous domain. This discrete nature will also affect the intermediate correspondences established and hence the final results. Moreover, the discrete nature of the optimization process and its conventional operation strategy also results in ambiguous problem of the forward and backward registration process. So in order to obtain a source-destination symmetric transformation pair, the inverse consistent constraint cannot be omitted.

3.4 Role of Inverse Consistency in Registration

As we have mentioned in the above section, the forward and backward registration process will generate an ambiguous transformations result. It is necessary to constrain the forward and backward registration process together in order to achieve the consis-

tent property. So what does source-destination symmetry or consistency mentioned above imply in a simple 1D registration problem and when will it be good to the registration result? Actually in 1D case, enforcing inverse consistency in a deterministic sense means the hill climbing process should be initialized in both direction with the same step length and same starting point, i.e. evaluate the matching criteria in pairwise nature: $(1,-1)$, $(2,-2)$... $(n,-n)$ together for the testing signal over the reference signal. Equivalently, there would be a new matching criteria curve that is a combination of the forward and backward matching criteria curve. The simplest way is to have a non-weighted linear combination [23], which can be obtained simple addition, as shown in Fig.3.1(e),(f), Fig.3.2(e) and (f). Here, a critical rule for combining the forward and backward matching criteria curves under deterministic sense is that they should be combined in the corresponding transformation position, i.e. the NMI_f value at 0.5 translation must be combined with the NMI_r value at 0.5 translation also.

It should be noted that imposing a deterministic consistent constraint will not always result in better registration results. In Fig.3.2(f) , although the relative height of the wrong peaks are decreased by summing up the forward and reverse registration criteria curves, the new matching criteria still give the same wrong maxima $(-1,1)$. Deterministic consistency will only give better registration results if the wrong peaks in the forward and backward matching criteria curve are eliminated and a new peak closer to the ground truth transformation is established. In Fig.3.2(e), the transformation pair corresponding to optimum will be around $(-0.8,0.8)$ which is unambiguous instead of $(-1.1,-0.5)$ and also closer to the ground truth $(-0.5,0.5)$. In terms of physical anatomy, combining the two matching criteria curves to obtain a better registration results can be linkened to interference in wave phenomena destructive interference is formed at the wrong peak position and constructive interference at the peak position nearer to the ground truth [5].

As stated above, source-destination symmetry in deterministic sense means that the combination of the forward and backward registration curves have to be in fixed corresponding transformation position, i.e., the NMI_f value at 0.5 translation have to combine with the NMI_r value at 0.5 translation (remember the pairwise nature

$(-1,1), \dots, (-n,n)$). This means we are still trusting the matching criteria. However, as we have shown above due to inadequate sampling, the registering objects cannot fully represent their original continuous objects so that the matching criteria cannot reflect the real ground truth. As a result, we believe that if a relaxation of the fixed combination between the two curves is allowed, there will be a mean to achieve better registration results through consistency.

This relaxation of the fixed combination means combining the 2 curves in some stochastic fashion instead of deterministic one, i.e., sliding the 2 curves before combination (e.g. imagine the value at -1.5 translation from the NMIc curve can be come from the value at -1.3 translation in the NMIf curve and the value at -1.6 translation in the NMIr curve). This makes it more likely that distinct destructive interference on the wrong peaks. In turn, this increases the potential means for the inverse consistent constraint to make the registration results closer to the underlying ground truth (make a more distinct destructive interference on the wrong peaks). The range of the sliding of the two curves should not be the same as the resultant transformation error between the forward and backward registration process is not necessary equal. Therefore, if we can stochastically impose the sliding range of the forward and backward matching criteria curves or equivalently, consider the errors associated with the transformation matrices individually during the combination, there is another mean to achieve a better registration result.

Chapter 4

Stochastic Inverse Consistency

4.1 Introduction

In this chapter, we will describe a new way to enforce inverse consistency in registration through our stochastic inverse consistency. As described in chapter 3, the matching criteria cannot result in the ground truth transformation due to the discrete nature of the information sources. This problem is not solve by the matching criteria since theoretically the function of matching criteria is to give maximum when the two objects are overlapped with maximal similarity in terms of the matching criteria. However, the matching criteria indeed fulfill its function as shown in the continuous case.

Therefore, the errors associated with the extracted transformations pair by any registration method should not be ignored. In that sense, one should have stochastic uncertainties associated with the transformation matrices when the inverse consistent constraint is enforced. In addition, the inherent imperfectness in the consistent constraint should also be taken into account at the same time as our ultimate goal to achieve source-destination symmetry or inverse consistency over the ground truth transformations instead of the transformations with maximal matching criteria value. Hence there will also be a stochastic uncertainty term incorporated with the inverse consistent constraint.

4.2 Stochastic Inverse Consistent Representation

As stated above, in this thesis we are arguing that rather than enforcing inverse consistency under deterministic and imperfect sense, we should model the consistent constraint with the simultaneous consideration of the underlying stochastic uncertainties within the forward and backward transformation matrices and hence the imperfectness of the source-destination symmetric constraint. Thus our stochastic inverse consistent model becomes:

$$(T_{12} + E_{T_{12}}) * (T_{21} + E_{T_{21}}) = I + R_i \quad (4.1)$$

where $E_{T_{12}}$ and $E_{T_{21}}$ model the stochastic error properties of the transformation matrix T_{12} and T_{21} . In this thesis, we test with 4-by-4 affine transformation matrices, in theory, we can also enforce the stochastic relationship on non-rigid deformation. R_i is the error imposed on the imperfectness of the consistent constraint. With this formulation, we can provide more flexibility on imposing source-destination symmetry between the forward and backward registration processes, without compromising accuracy.

It is easy to notify that the error matrices E and the transformation matrices govern the 'individual sliding range of the matching criteria curve' while the R_i matrix is related to the 'degree of sliding' when combining the 2 curves together. Up to now we haven't enforce any deterministic weighting between the matching criteria value on the 2 curves to avoid any fixed bias. In potential investigations we may deal with the weighting when we combine the 2 curves together. However, notice that even without any weighting, sliding the 2 curves already fulfill the goal to 'destruct the wrong peaks' completely.

In this thesis, we have adopted simple derivations of the error matrices and set them as the differences between the transformation matrices and their respective inverse of the corresponding reverse transformation matrices i.e. :

$$E_{T_{12}} = |T_{12} - T_{21}^{-1}| \quad E_{T_{21}^{-1}} = |T_{21} - T_{12}^{-1}| \quad (4.2)$$

We adopted this simple assumption that the difference of the forward and inverse of the backward transformation has already set up a loose upper bound of the error as the final transformation solved under the stochastic inverse consistent model should be some way 'in-between' of the 2 input transformation matrices. For the R_i matrix, we simply assume all the entries will have the same stochastic property and set it as Δ_r such that $R_i \in R^{4 \times 4}$ with all the entries equal to Δ_r :

$$R_i = \begin{pmatrix} \Delta_r & \cdots & \cdots & \Delta_r \\ \vdots & \ddots & & \vdots \\ \vdots & & \ddots & \vdots \\ \Delta_r & \cdots & \cdots & \Delta_r \end{pmatrix} \quad (4.3)$$

To further simplify our current error model, we assume all the elements in the error matrices have zero mean and are independent of each other. The individual element of the error matrices, their relationship within the matrix and also the interrelation among the error matrices will be examined in future work. Once again, we are aiming at developing a completely new stochastic inverse consistent model in this thesis. The modelling of the error properties depends on the actual data and also the corresponding matching criteria which is very complicated. Also notice that the modelling of the stochastic properties will be the potential mean to improve the registration results through inverse consistency which will be investigated heavily in future work. These matrices will be involved in building the error equilibration matrices for the Generalized Total Least Solvers in the following section.

4.3 GTLS Formulation

After obtaining a pair of forward and backward transformations from any point set or image registration algorithm, our stochastic framework aims at considering the errors on the transformation matrices and imposing stochastic property on the inverse consistent constraint at the same time to optimally solve a pair of consistent transformation matrices. In order to solve the problem while considering all the errors

simultaneously, we adopt the total least square approach [31]. In addition, as the error on every entry do not carry the same stochastic property and some of the entries are error free, a Generalized Total Least Square (GTLS) [30] approach is used. The GTLS formulation is as follows: Consider a overdetermined system of linear equations with a set of m linear equations in $n \times d$ unknowns X :

$$AX \approx B \quad A \in R^{m \times n}, B \in R^{m \times d} \text{ and } X \in R^{n \times d}, m \geq n + d \quad (4.4)$$

$$\text{Partition } A = [A_1; A_2] \quad A_1 \in R^{m \times n_1}, A_2 \in R^{m \times n_2} \text{ and } n = n_1 + n_2 \quad (4.5)$$

$$X = [X_1^T; X_2^T]^T \quad X_1 \in R^{n_1 \times d} \text{ and } X_2 \in R^{n_2 \times d} \quad (4.6)$$

Assume that the columns of A_1 are error free and that nonsingular error equilibration matrices $R_D \in R^{m \times m}$ and $R_C \in R^{(n_2+d) \times (n_2+d)}$ are given such that the errors on $R_D^{-T}[A_2, B]R_C^{-1}$ are equilibrated, i.e. uncorrelated with zero mean and same variance. Then, a GTLS solution of (4.4) is any solution of the set

$$\widehat{A}X = A_1X_1 + \widehat{A}_2X_2 = \widehat{B} \quad (4.7)$$

where $\widehat{A} = [A_1, \widehat{A}_2]$ and \widehat{B} are determined such that

$$\text{Range}(\widehat{B}) \subseteq \text{Range}(\widehat{A}) \quad (4.8)$$

and

$$\| R_D^{-T}[\Delta \widehat{A}_2, \Delta \widehat{B}]R_C^{-1} \|_F = \| R_D^{-T}[A_2 - \widehat{A}_2, B_2 - \widehat{B}]R_C^{-1} \|_F \text{ is minimal} \quad (4.9)$$

The problem of finding $[\Delta \widehat{A}_2, \Delta \widehat{B}]$ such that Equ.(4.8) and (4.9) are satisfied is referred to as the GTLS problem. Whenever the solution is not unique, GTLS singles out the minimum norm solution, denoted by $\widehat{X} = [\widehat{X}_1^T; \widehat{X}_2^T]^T$.

Our objective is to formulate our problem into the GTLS formulation and solve the fitting transformation matrix under the consideration of the transformation errors and the errors on the consistent constraint simultaneously by making use of the

in Equ.(4.7). Hence the GTLS formulation of our stochastic inverse consistent model becomes:

$$\begin{bmatrix} Q_{12} \\ invQ_{21} \end{bmatrix} X \approx \begin{bmatrix} I \\ I \end{bmatrix} \quad \begin{bmatrix} invQ_{12} \\ Q_{21} \end{bmatrix} Y \approx \begin{bmatrix} I \\ I \end{bmatrix} \quad (4.14)$$

Where X and Y are the optimal forward and backward transformation matrices respectively, both containing the information from the original T_{12} and T_{21} . In order to get back the forward and backward transformation T_{12}^* and T_{21}^* , we simply perform the permutation and transpose on the GTLS solutions X and Y :

$$T_{21}^* = (P * X)^T \quad T_{12}^* = (P * Y)^T \quad (4.15)$$

Apart from the input transformation matrices, the error properties are also necessary to specify the GTLS formulation. The error matrix $E_{Q_{12}}$ for Q_{12} and $E_{invQ_{12}}$ for $invQ_{12}$ are derived as presented in Equ.(4.2) i.e.

$$E_{Q_{12}} = |Q_{12} - invQ_{21}| \quad E_{invQ_{12}} = |Q_{21} - invQ_{12}| \quad (4.16)$$

and the first column is dropped as the first column of Q_{12} is error free. The error matrices $E_{invQ_{21}}$ and $E_{Q_{21}}$ transformation matrix are formed respectively by:

$$E_{invQ_{21}} = \frac{(1 - \alpha)}{\alpha} * E_{Q_{12}} \quad E_{Q_{21}} = \frac{(1 - \alpha)}{\alpha} * E_{invQ_{12}} \quad (4.17)$$

where α is the weighting on the error of the forward transformation matrix T_{12} (assume signal with higher resolution be the testing signal):

$$\alpha = \frac{\text{voxel size of } I_1}{\text{voxel size of } I_2} \quad \text{or} \quad \alpha = \frac{\# \text{ of points in point set 2}}{\# \text{ of points in point set 1}} \quad (4.18)$$

So by imposing the above relationship, the registration result with a higher resolution test image or point matching result with more points in the test point set will be more trusted. While in this thesis we use this simple assumption to model the weighting function between the error on forward and backward registration results from two

images under different resolutions, more complicated way can be investigated and is a possibility of future work.

The error equilibration matrices R_C and R_D are then formed from the square root of the error covariance matrices C and D:

$$C = \Delta^T \Delta \quad \text{and} \quad D = \Delta \Delta^T$$

$$\text{where } \Delta = \begin{bmatrix} E_{Q_{12}} & R_i \\ E_{invQ_{21}} & R_i \end{bmatrix} \quad (4.19)$$

The matrix Δ above represents the stochastic property of the error in the linear system for solving X in Equ.(4.14). After deducing C and D, R_C and R_D for the input of the GTLS solver are simply obtained from their Cholesky decomposition, i.e. $C = R_C^T R_C$ and $D = R_D^T R_D$. Notice that the Δ matrix in solving Y in Equ.(4.14) is:

$$\Delta = \begin{bmatrix} E_{invQ_{12}} & R_i \\ E_{Q_{21}} & R_i \end{bmatrix} \quad (4.20)$$

4.4 Inverse Consistency by Iterative GTLS Solution

After defining the GTLS model to fit the transformation matrix based on the stochastic inverse consistency, we set up the whole iterative process from the registration results T_{12} and T_{21} in order to extract both the forward transformation matrix T_{12}^* and the backward transformation matrix T_{21}^* . Recall that these matrices are inverse of each other. The input for the iteration process is Q_{12} , Q_{21} , $invQ_{12}$ and $invQ_{21}$ in Equ. (4.10) and (4.11).

$$\begin{bmatrix} Q_{12}^{(0)} \\ invQ_{21}^{(0)} \end{bmatrix} X^{(0)} \approx \begin{bmatrix} I \\ I \end{bmatrix} \quad \begin{bmatrix} invQ_{12}^{(0)} \\ Q_{21}^{(0)} \end{bmatrix} Y^{(0)} \approx \begin{bmatrix} I \\ I \end{bmatrix} \quad (4.21)$$

with the corresponding stochastic property in the noise data:

$$\begin{bmatrix} E_{Q_{12}}^{(0)} & R_i \\ E_{invQ_{21}}^{(0)} & R_i \end{bmatrix} \quad \text{and} \quad \begin{bmatrix} E_{invQ_{12}}^{(0)} & R_i \\ E_{Q_{21}}^{(0)} & R_i \end{bmatrix} \quad (4.22)$$

the '0' in the brackets is the number of iteration and the solved $X^{(0)}$ and $Y^{(0)}$ are:

$$X^{(0)} = P^{-1} * (T_{21}^{(1)})^T \quad Y^{(0)} = P^{-1} * (T_{12}^{(1)})^T \quad (4.23)$$

so

$$(X^{(0)})^{-1} = invQ_{21}^{(1)} \quad \text{and} \quad P * (X^{(0)}) * P = Q_{21}^{(1)} \quad (4.24)$$

$$(Y^{(0)})^{-1} = invQ_{12}^{(1)} \quad \text{and} \quad P * (Y^{(0)}) * P = Q_{12}^{(1)} \quad (4.25)$$

The corresponding error matrices for the transformation matrices are also updated during the iteration, i.e., getting $E_{Q_{12}}^{(1)}, E_{Q_{21}}^{(1)}, E_{invQ_{12}}^{(1)}, E_{invQ_{21}}^{(1)}$ by Equ.(4.16) and (4.17) to fit the input matrices of the GTLS solvers. Notice the transformation errors should be smaller during the iteration (closer to the ground truth) while the error matrix R_i for the consistency constraint is fixed since the initial input stochastic inverse consistent model is kept unchanged.

Therefore all the components for the GTLS solvers are updated and the process can be repeated until the consistency error (e) is less than a given threshold:

$$\|(P * X^{(n)})^T * (P * Y^{(n)})^T - I\|_F = e < \text{threshold} \quad (4.26)$$

and the GTLS solution matrices will be:

$$T_{21}^* = (P * X^{(n)})^T \quad T_{12}^* = (P * Y^{(n)})^T \quad (4.27)$$

Notice that from Equ.(4.26) and (4.27), the final output matrices T_{12}^* and T_{21}^* from the GTLS system are perfect inverse of each other. Therefore, the objective to derive

a novel model for source-destination symmetric registration in this thesis is achieved.

Chapter 5

Experiments and Discussions

5.1 Introduction

Experiments have been performed on synthetic image data, point set data and real MRI brain images. The forward and backward registration results of all the experiments are shown and used as the input for our stochastic inverse consistency model to achieve inverse consistency. Different kinds of data and matching algorithm were applied so that it showed the robustness of stochastic inverse consistency on different types of registration problems. The main purpose of the experiments on synthetic images data and real images data is to provide visual results of the algorithm. Meanwhile the point set data serves as a robustness evaluation through error distance measurements.

5.2 Experiments on Synthetic Image Data

Synthetic image data with known transformation and noise levels were used to verify the effects of the stochastic inverse consistency on the forward and backward transformation results. The effect of trusting the registration process with a higher resolution testing image is shown in the second example.

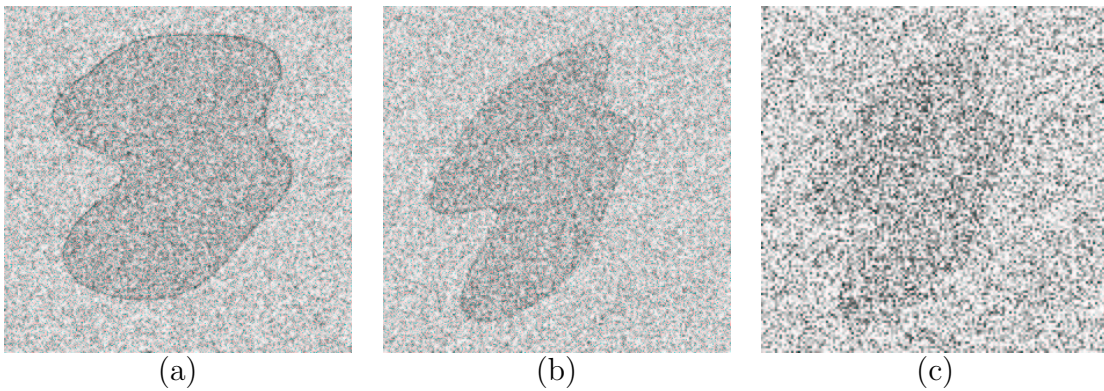


Figure 5.1: (a): Image A. (b): Image B. (c): Image C: Image B downsampled by 2 in x and y dimensions.

5.2.1 Data Description

A known affine transformation was applied on 2D synthetic image A to form another image B, then image B is downsampled by 2 in x and y dimension to form image C. Noise is added to all the images. Image A and B form the first registering pair (Fig.5.1(a) and (b)) while image A and C form another registering pair (Fig.5.1(a) and (c)).

5.2.2 Results and Discussions

In the synthetic image example, the forward and backward registration is performed by utilizing the Normalized Mutual Information (NMI) [24] to extract T_{12} and T_{21} . These two matrices and their inverses are passed to the GTLS system to obtain a pair of source-destination symmetric transformation pairs T_{12}^* and T_{21}^* .

The results for registering image A and image B are shown in Fig.5.2. In Fig.5.2(a)-(c), the transformations representing the forward warping results shown by the warped red contours over image B. The red contours are the warped boundary of the object in image A by different transformations, from left to right, are $T_{12}, T_{12}^*, T_{21}^{-1}$. In Fig.5.2(d)-(f), the results for the backward process are illustrated. The warped contours from the object's boundary in image B is overlaid on image A. The transformations for the warping of image B, from left to right, are $T_{12}^{-1}, T_{21}^*, T_{21}$. In this example, we can observe that the GTLS solution actually gives a better registration results due to the cancellation of opposite bias from the forward and backward registration

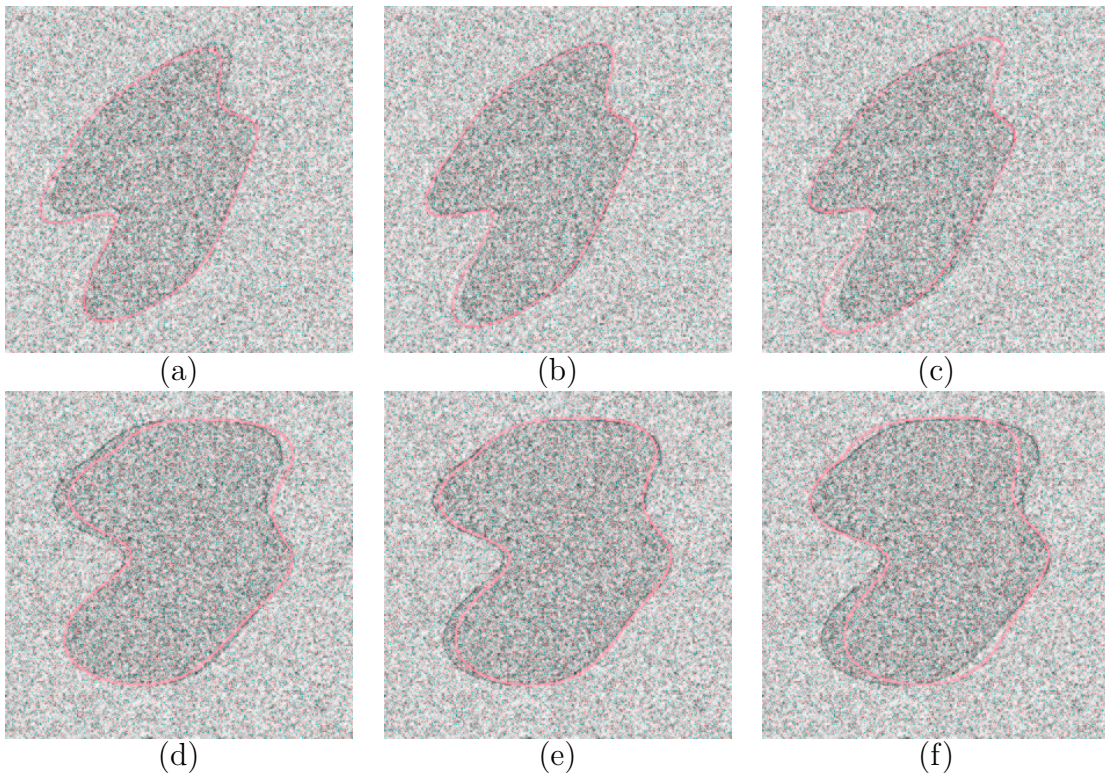


Figure 5.2: (a)-(c): transformations represented the forward warping results, left to right: $T_{12}, T_{12}^*, T_{21}^{-1}$. (d)-(f): transformations represented the backward warping results, left to right: $T_{12}^{-1}, T_{21}^*, T_{21}$. The red contours are the warped boundary of the object in image A for row 1 and image B for row 2 with the warping by the transformations specified above.

results.

Fig.5.3 shows the registering results of image A with a lower resolution image C. This example also tests the effect of the alpha value in Equ.(4.17). From Equ.(4.18), the alpha value is set to 0.25. As the same order in Fig.5.2, the first row has forward transformation results: $T_{12}, T_{12}^*, T_{21}^{-1}$. The second row has the backward transformation results: $T_{12}^{-1}, T_{21}^*, T_{21}$. Although in this example, the GTLS solutions are not the best, but the results are closer to the better one instead of the worse one, e.g, the backward transformation results illustration in Fig.5.3(d)-(f), T_{21}^* is closer to T_{12}^{-1} instead of T_{21} .

5.3 Experiments on Point Sets Data

The point set data performs the robustness evaluation of our GTLS solution. The registration error is measured by the sum of squared distances (SSD) between the

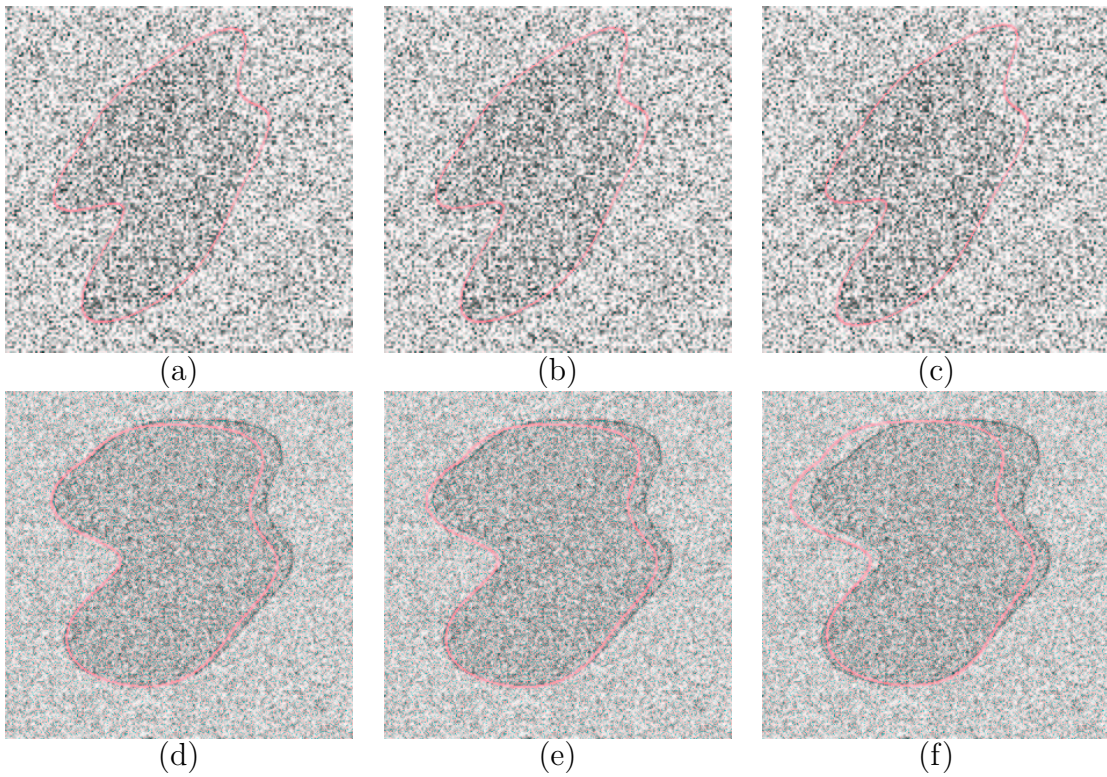


Figure 5.3: (a)-(c): transformations represented the forward warping results, left to right: $T_{12}, T_{12}^*, T_{21}^{-1}$. (d)-(f): transformations represented the backward warping results, left to right: $T_{12}^{-1}, T_{21}^*, T_{21}$. The red contours are the warped boundary of the object in image A for row 1 and image C for row 2 with the warping by the transformations specified above.

coordinates of the reference point set and the warped test point set by different transformations.

5.3.1 Data Description

We begin with a simple example, a point set representing a fish to illustrate general point matching problem. Then point sets representing different human brains are tested to demonstrate its use in medical image analysis. All the examples will be driven by a testing point set and the corresponding reference point set. The reference point set is formed by applying known non-rigid transformation on the testing point set and then adding noise to both point sets or outliers to the reference point set.

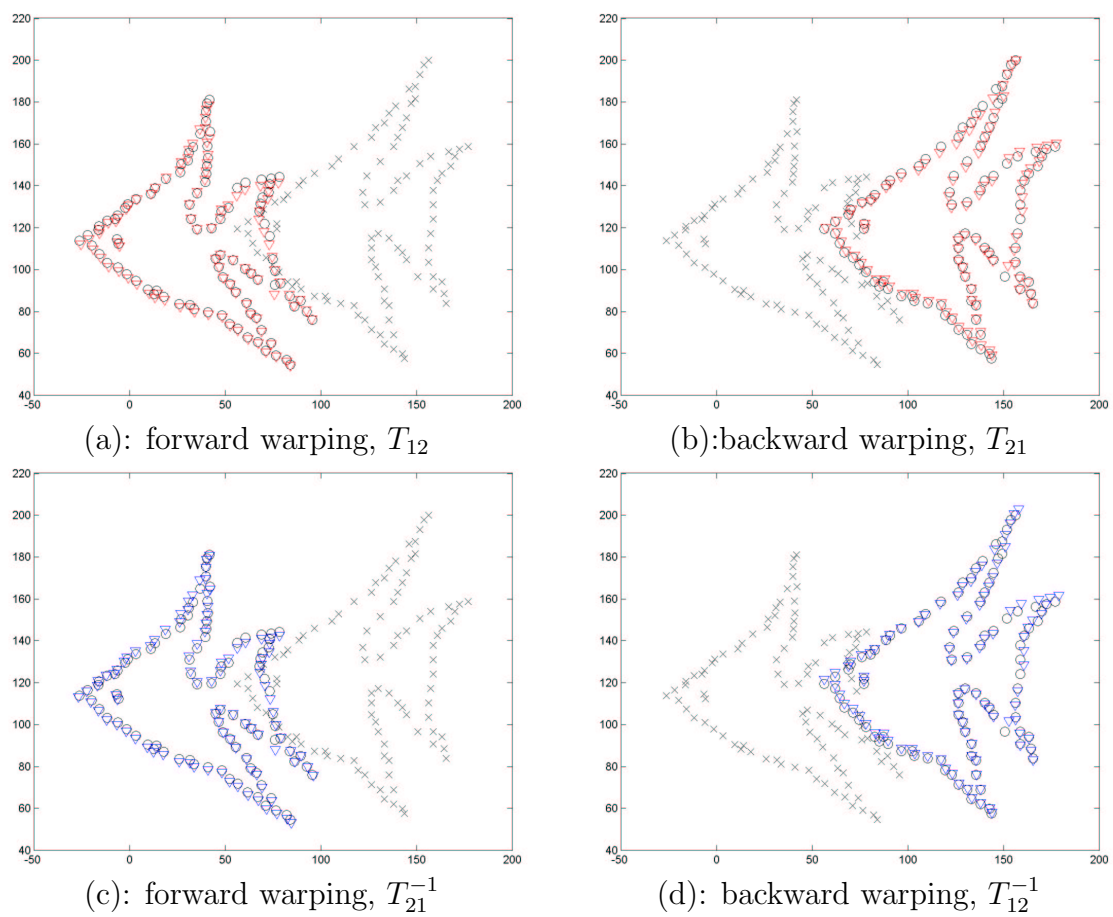


Figure 5.4: Registering black crosses to black circles. Left column and right column represent the forward and backward registration process respectively. The red or blue triangles above are the warping results from the transformations specified below the corresponding figures.

5.3.2 Results and Discussions

The forward and backward point matching results for the fish example are shown in Fig.5.4. The point matching algorithm we applied for the point matching process is the robust point matching algorithm RPM [21], the fish point sets are modified from their web-site. Then the T_{12} and T_{21} and their inverses are used as the input of our GTLS system. The final GTLS results with the input transformations are shown in Fig.5.5. The GTLS solutions are inverse consistent and in-between the input forward and backward transformations (from the positions of the green stars). Table.5.3.1 shows the SSD between the coordinates of the reference point set and the warped test point set with different transformations. As shown in the table, the GTLS solutions outperform the input transformations with a smaller SSD.

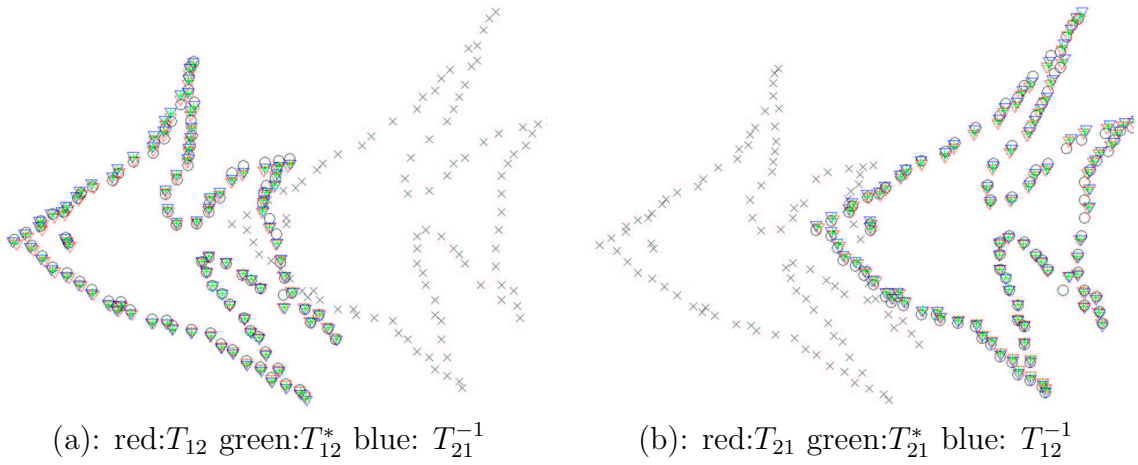


Figure 5.5: (a) and (b) are the results for the forward and backward point matching processes respectively. The red and blue triangles and the green stars are the warping results of the black crosses by the transformations specified in the corresponding figures.

Position Errors			
Forward Matching		Backward Matching	
Transformation	SSD	Transformation	SSD
T_{12}	282.47	T_{21}	428.45
GTLS T_{12}^*	262.27	GTLS T_{21}^*	386.85
T_{21}^{-1}	303.08	T_{12}^{-1}	427.94

Table 5.1: Sum of squared distances (SSD) from different transformations results.

The fish example gives a sense about how the point set data experiments are performed and evaluated. More point set example are tested with our stochastic inverse consistency as illustrated below. The brain images for the brain point set data are from the BrainWeb project [1]. Points are extracted from the brain images with canny edge detector [6], then the edge points are clustered until a reasonable amounts of points remain to form the testing point sets. Different degree of non-rigid transformations are applied to the testing point sets to form the reference point sets. The positions of points in both point sets are perturbed by zero mean gaussian noise with different standard deviation. Different amounts of outliers are also added to the reference point sets to make the point matching process obtaining a worse results. These are performed for evaluation of our stochastic inverse consistent model under worse input conditions.

Fig.5.6 shows the first brain point set example. As described above, the blue circles are the points extracted to be the testing point set, while the black crosses are

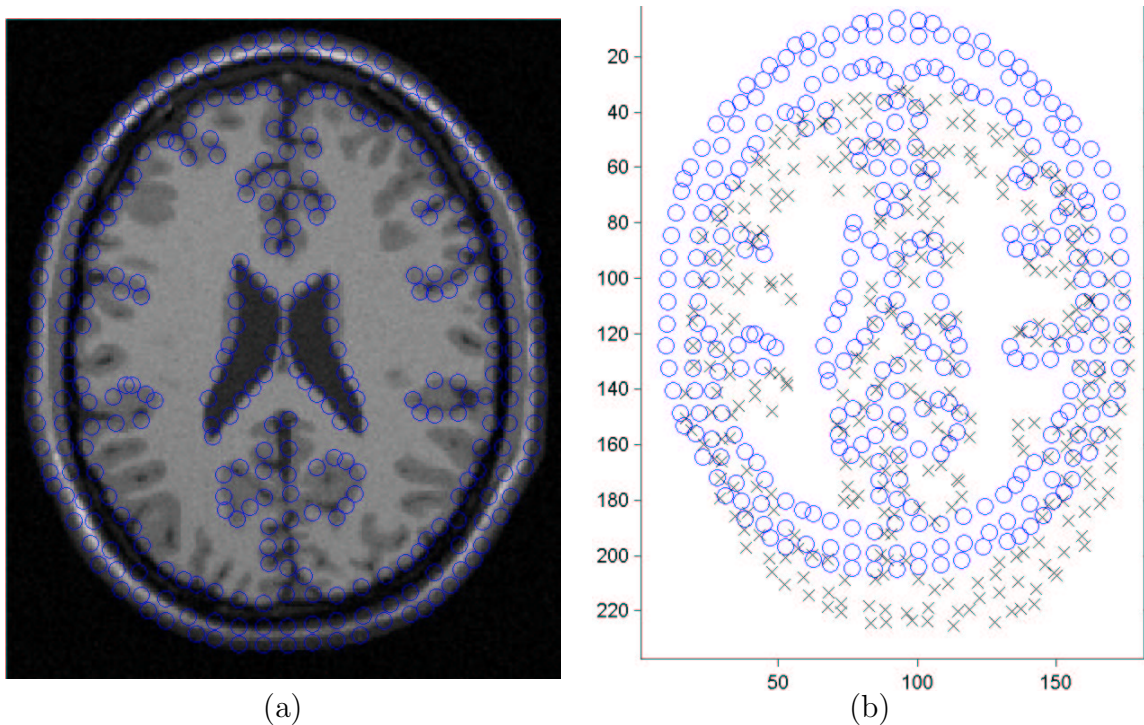


Figure 5.6: (a): Brain image with the extracted point sets. (b): Testing point sets (blue circles) with the reference point sets (black crosses).

the reference point set. The points shown in Fig.5.6 were not perturbed by noise or outliers. The visual results and the numerical error of the transformation in terms of SSD is shown in Fig.5.7. In these figures, the GTLS solutions solved are in-between their inputs. The plots show that in this example the GTLS solutions are better than their inputs most of the time. Even the GTLS solution is not the best, it is still closer to the input with the best result as shown in Fig.5.7(c) (standard deviation = 4).

Similar experiments are performed on another brain image. The point sets input are shown in Fig.5.8. The results for the forward and backward registration processes are shown in the left and right rows of Fig.5.9 respectively. The plots in Fig.5.9(c) and (d) do not show the obvious trend as those in Fig.5.7. However, an interesting result is obtained at standard deviation = 5 in the plots. At that point, one of the transformation results is particular poor (T_{12}/T_{12}^{-1}). Although our GTLS solution is not the best at that point, but it is very close to the best result instead of the worst one.

In the last brain point sets example, we extract points from a brain image similar to the one in first example, Fig.5.10. Small and large deformations are applied on

the testing point set to form two different reference point sets, in Fig.5.11(a) and (b). Examples of the point sets with addition of noise or outliers are shown in Fig.5.11(c) and (d). The visual results and results for error are shown in Fig.5.12 and Fig.5.13. The results show similar pattern with the above examples. The GTLS solution either outperforms the input transformation matrices or even if it is not the best, it will close to the input with a better performance. In this example we also examine the consistency error by comparing the terms $\| T_{12} * T_{21} - I \|_F$ for the input forward and backward transformations pair and $\| T_{12}^* * T_{21}^* - I \|_F$ for the GTLS outputs. As shown in Fig.5.14, the GTLS outputs are guaranteed to be inverse consistent by Equ.(4.26) such that $T_{12}^* * T_{21}^*$ is equal to identity.

5.4 Experiments on Real Image Data

We also test our stochastic inverse consistent model with real images data. The images we used are from the Vanderbilt Retrospective Registration Project [33]. We pick out two slices from two different patients to test our model.

5.4.1 Data Description

The images we tested are two PD-weighted MR images from two different patient. Fig.5.15 shows the two input images. We define the forward registration process as registering I_2 to I_1 .

5.4.2 Results and Discussions

The visual results are shown in Fig.5.16. The forward and backward registration results are again derived from normalized mutual information as in the synthetic image example. From the red and blue contours, we can observe inconsistency in the forward and reverse processes, i.e., $T_{12} \neq T_{21}^{-1}$. Since there is no ground truth for error evaluation, we cannot determine the registration error numerically. However, from Fig.5.16(a) and (b), there are obvious registration errors as indicated by the

red ellipses. Such errors are not discovered in the GTLS results. All the registration results are displayed together in Fig.5.17 for comparison.

5.5 Convergency Issue

We have plotted the value for the consistency error (e) in Equ.(4.26) in every iteration during the iterative process. It is done in order to investigate the convergency property of the iterative process. The plot of consistency error (e) versus the number of iteration is the convergency profile (CP). The convergency profiles are plotted for the brain point sets experiment with all the combinations: small/large deformation + perturbed by noise/outliers(impulse noise). Examples for the convergency profile in each combination are shown in Fig.5.18. We did not show out all the convergency profiles for different amounts of noise and outliers. But an interesting fact is that for the case of deformation perturbed by noise, the number of iterations (3 in this case) for the whole process is the same under different amounts of noise. While for the deformation perturbed by outliers, the number of iterations under different amounts of outliers is also the same (4 in this case). These are the observations obtained from all the experiments on the brain point sets. Since not all the convergency profiles for different amounts of noise or outlier proportion are shown, the mean value of the convergency profile (from different amounts of noise or outliers) in each combination is shown in Fig.5.19 (together with the maximum value, minimum value and +/- 1SD from the mean value). From these figures, we can observe that after the first iteration, the numerical result of the value for evaluating Equ.(4.26) already becomes very small and the whole process terminates within 3 more iterations. The threshold is 10^{-6} in Equ.(4.26) for the brain point sets experiment. We zoom in the convergency profile in the second iteration to show the numerical result is very small in Fig.5.20. As it is difficult to illustrate the change of the convergency profile after the second iteration, the percentage change of the convergency error for the convergency profile is plotted in Fig.5.21. From the figures, it should be noticed that the percentage change is very large between every iteration, making the whole iterative process converge in

few iterations.

Among all the experiments on the brain point sets, the whole iterative process converge without any problems, i.e., the convergency profile is monotonic decreasing. However, we find an example which the convergency profile is oscillated. It is shown in Fig.5.22, the input transformation matrices are from the point matching results which are shown in Fig.5.23. In this example, the initial condition is very bad so that the 2 input matrices are very bad inverse of each other. In this thesis the relationship of the initial condition and the result of the convergency profile is not studied, but further analysis of the convergency issue will be one of our future work.

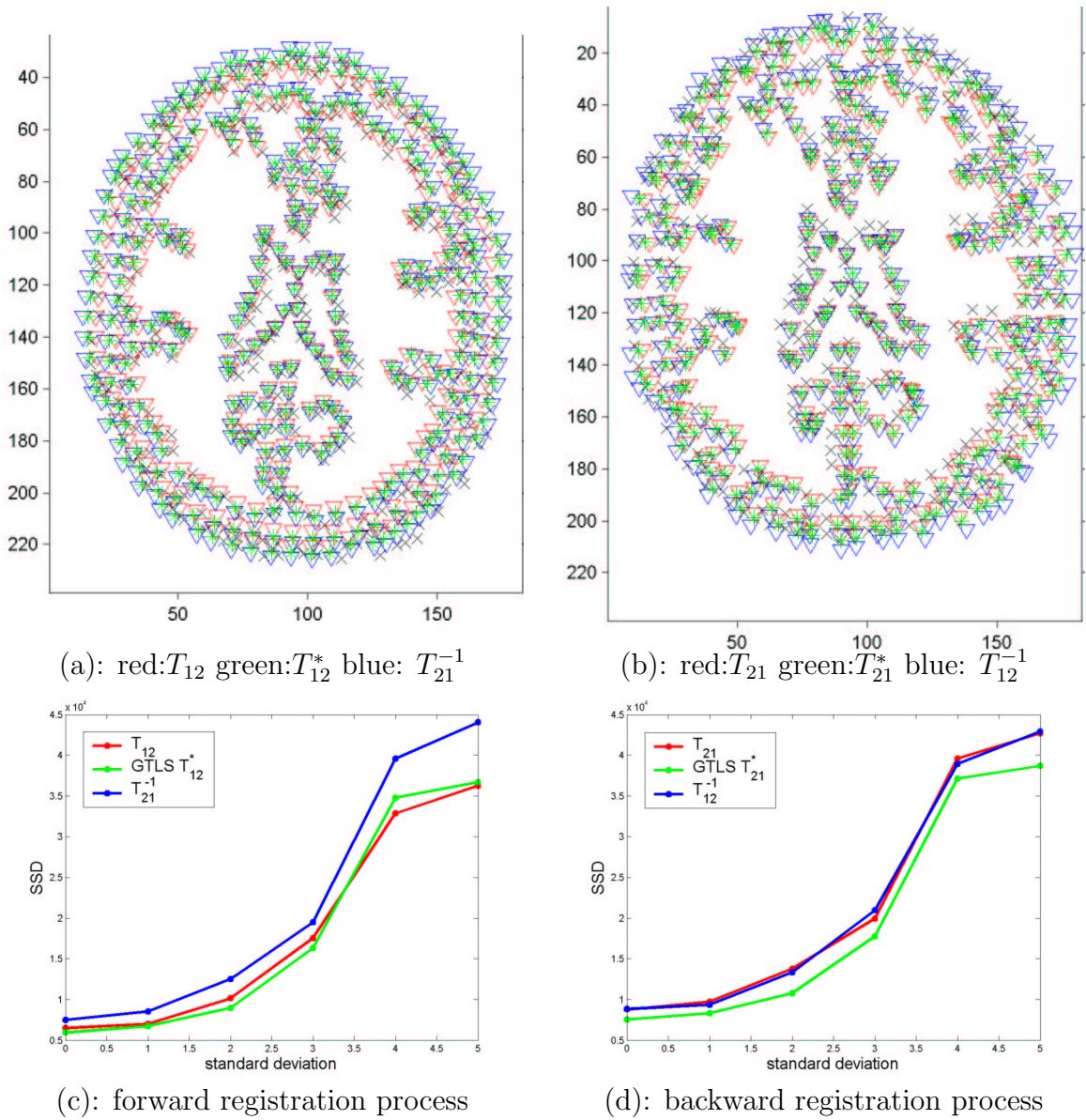
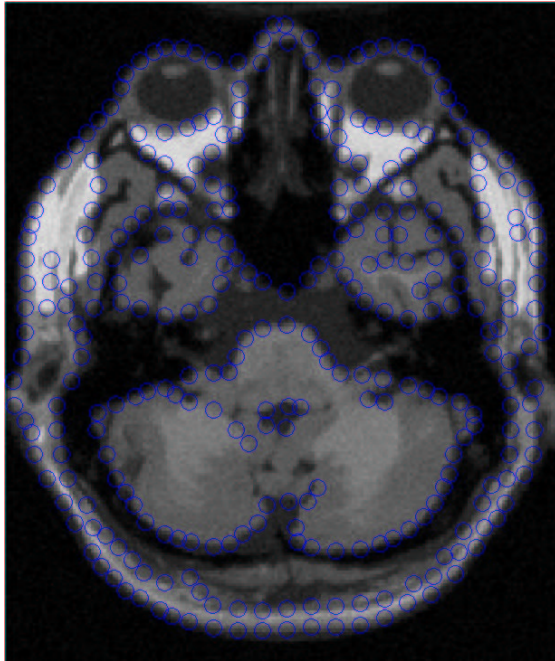
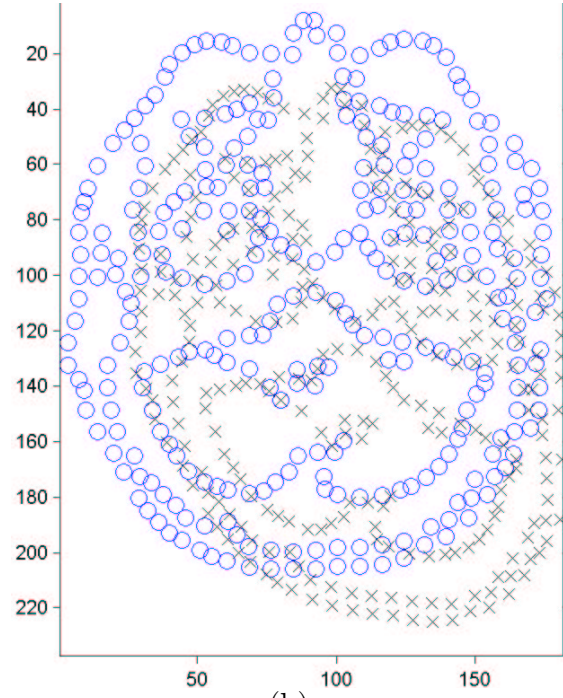


Figure 5.7: (a) and (b) are the visual results for the forward and backward point matching processes respectively. The red and blue triangles and the green stars are the warping results of the black crosses by the transformations specified in the corresponding figures. (c) and (d) are the plots of the sum of squared distances (SSD) for input point sets with different standard deviation of gaussian noise.

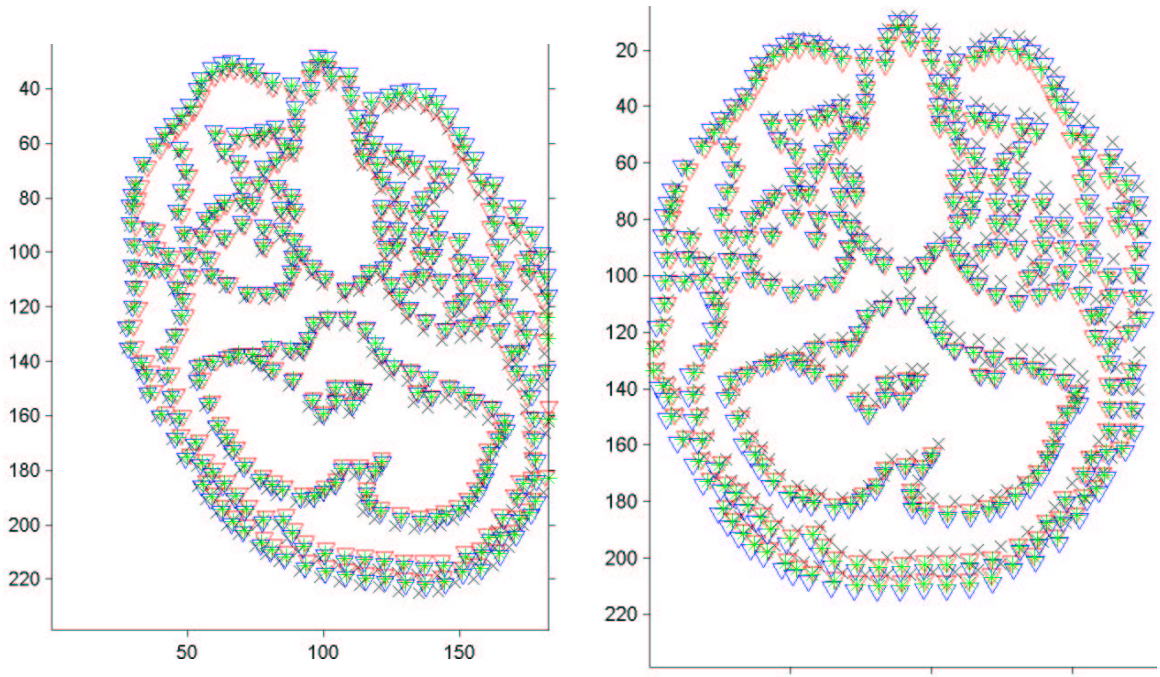


(a)



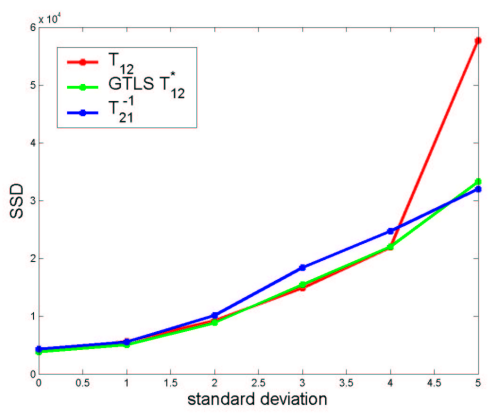
(b)

Figure 5.8: (a): Brain image with the extracted point sets. (b): Testing point sets (blue circles) with the reference point sets (black crosses).

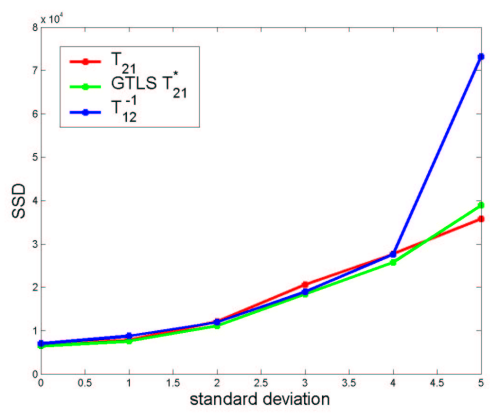


(a): red: T_{12} green: T_{12}^* blue: T_{21}^{-1}

(b): red: T_{21} green: T_{21}^* blue: T_{12}^{-1}



(c): forward registration process



(d): backward registration process

Figure 5.9: (a) and (b) are the visual results for the forward and backward point matching processes respectively. The red and blue triangles and the green stars are the warping results of the black crosses by the transformations specified in the corresponding figures. (c) and (d) are the plots of the sum of squared distances (SSD) for input point sets with different standard deviation of gaussian noise.



Figure 5.10: Brain image with the representing point set.

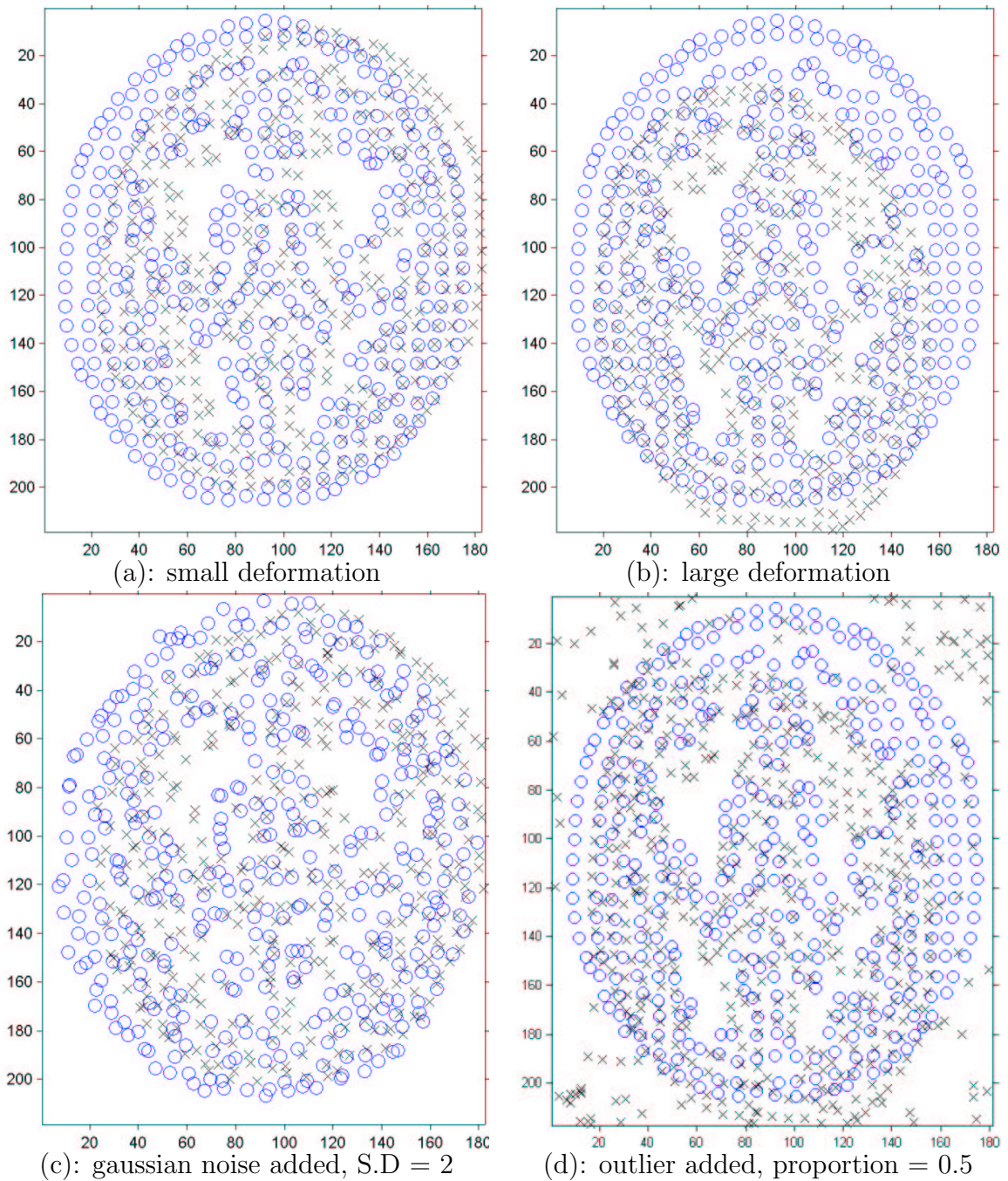


Figure 5.11: Column 1 and 2 are examples of small deformation and large deformation respectively. (a),(b) are the point set without any noise and outliers. In (c), positions of the points are perturbed by gaussian noise with standard deviation = 2. In (d), outliers are added to the reference point set.

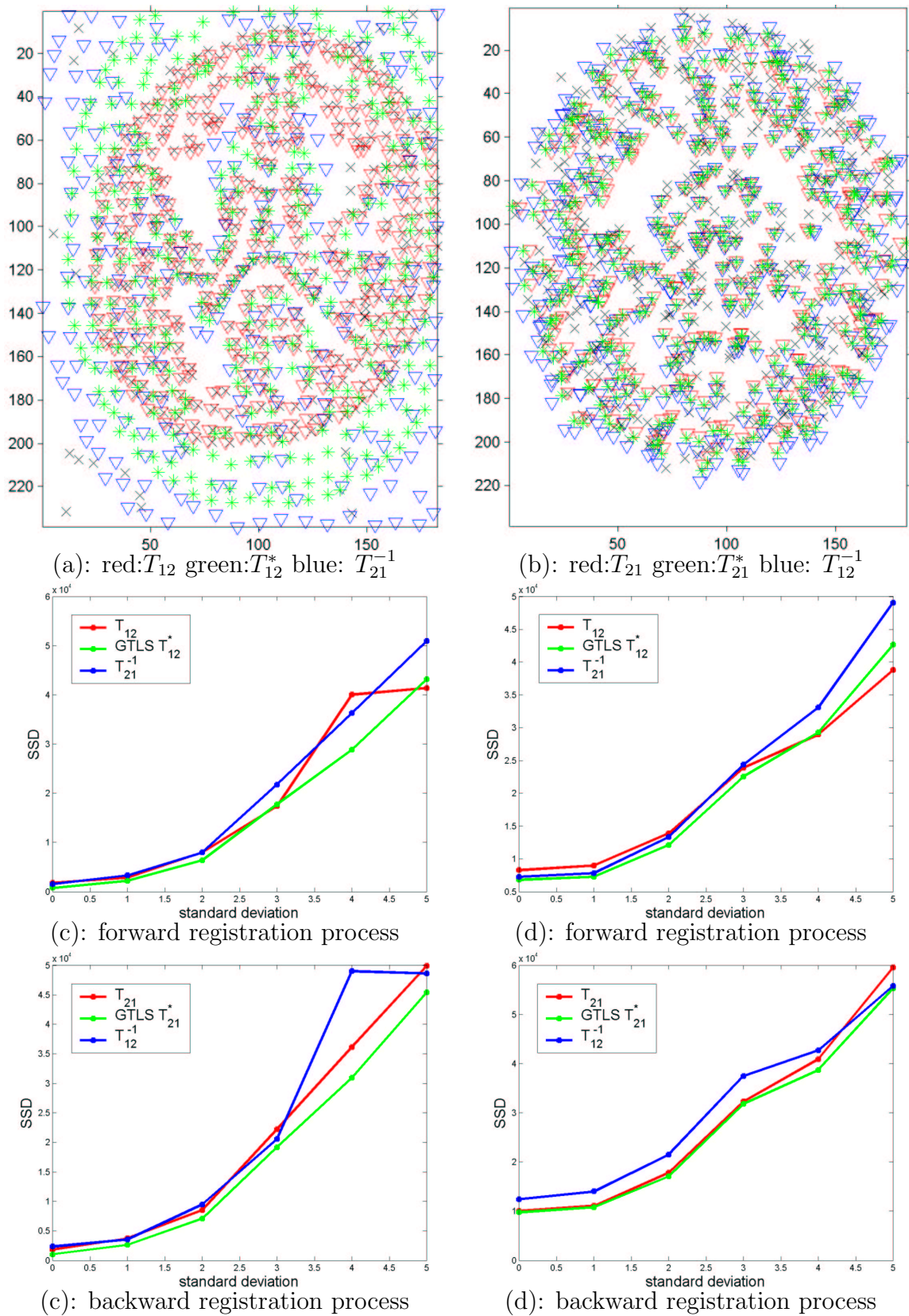


Figure 5.12: Column 1 and 2 are the results for registering reference point sets with small and large deformation respectively. (a) shows forward registration results for small deformation with outlier proportion = 0.1. (b) shows the backward registration results for large deformation with gaussian noise of S.D = 4 added. (c)-(f) are the plots of the sum of squared distances (SSD) for input point sets with different standard deviation of gaussian noise. While (c),(d) are for the forward registration process, (e),(f) are for the backward one.

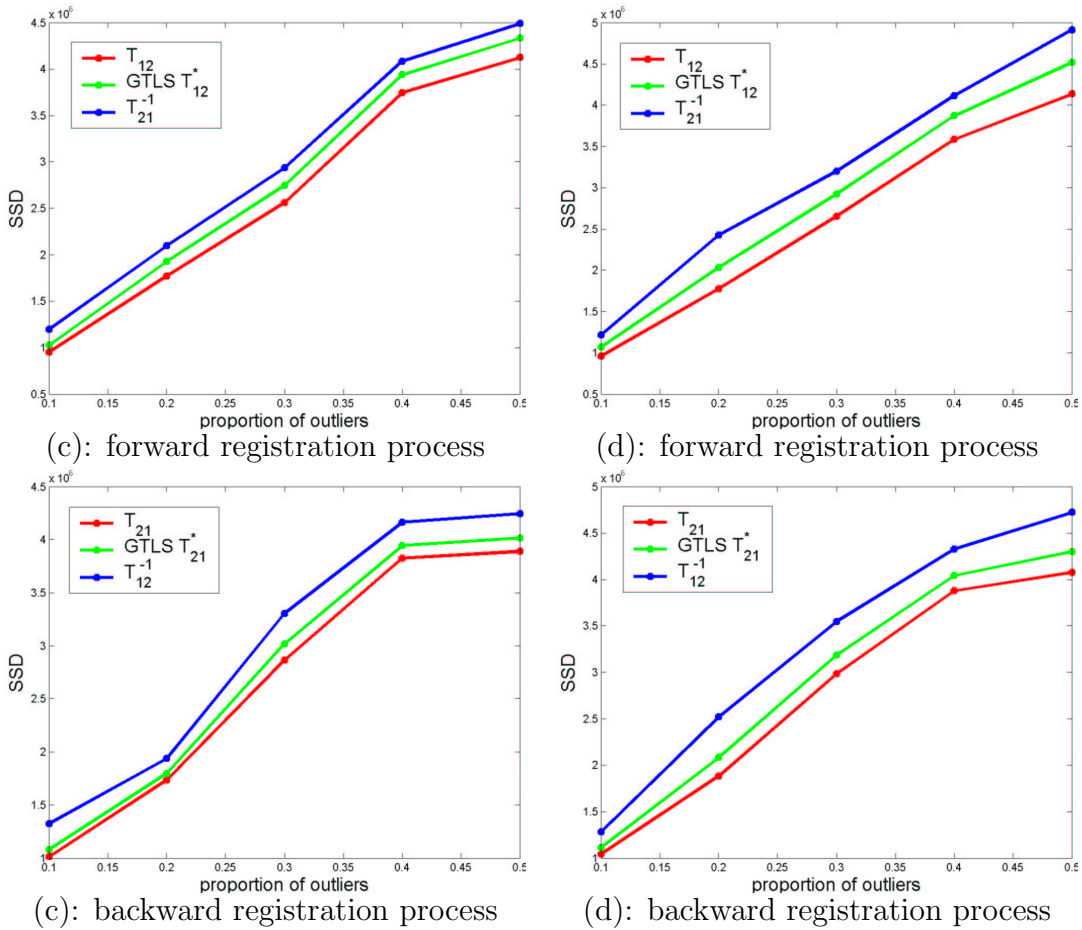


Figure 5.13: Column 1 and 2 are the results for registering reference point sets with small and large deformation respectively. (a)-(d) are the plots of the sum of squared distances (SSD) for input point sets with different proportion of outliers added. While (c),(d) are for the forward registration process, (e),(f) are for the backward one.

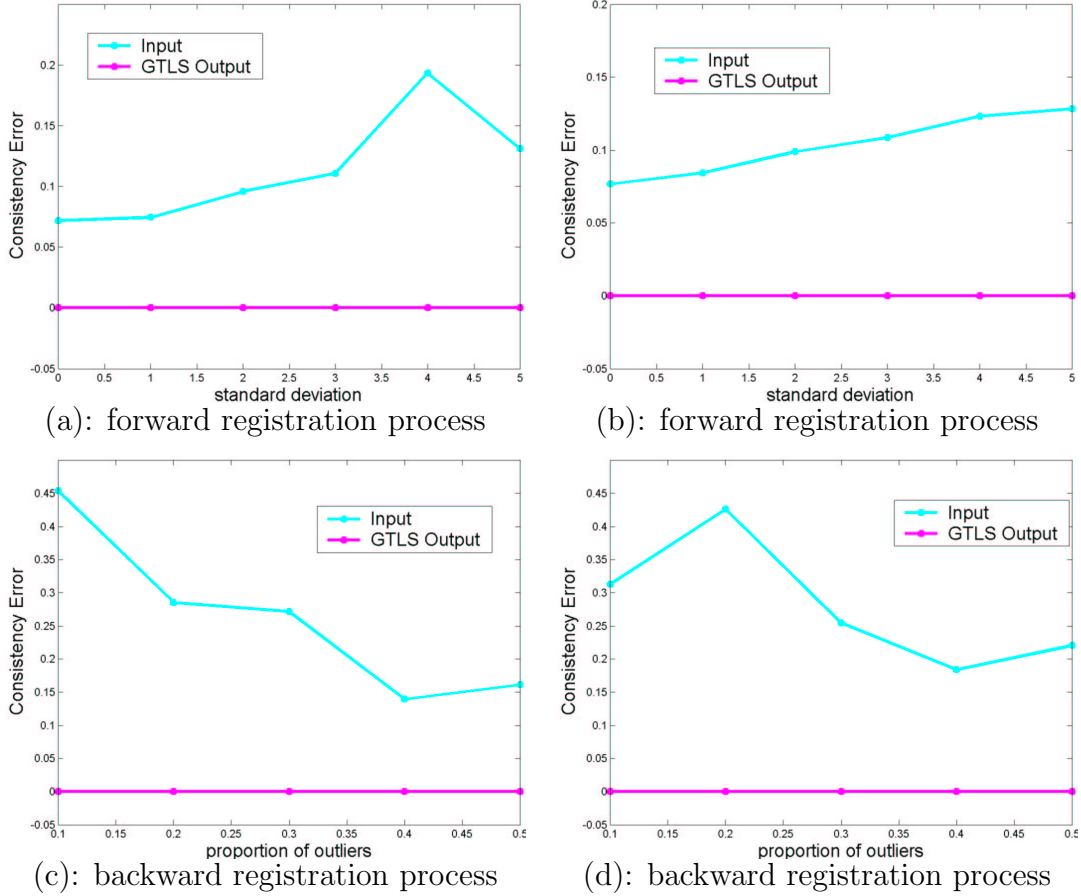
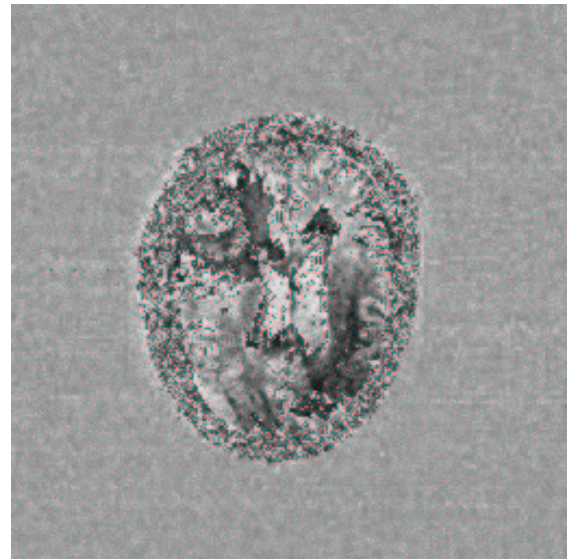
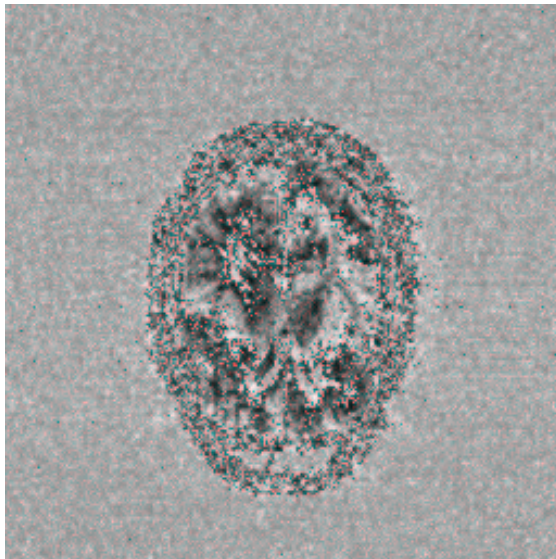
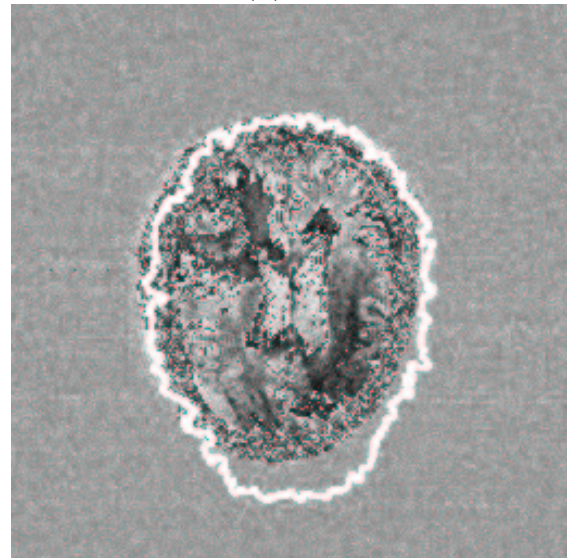
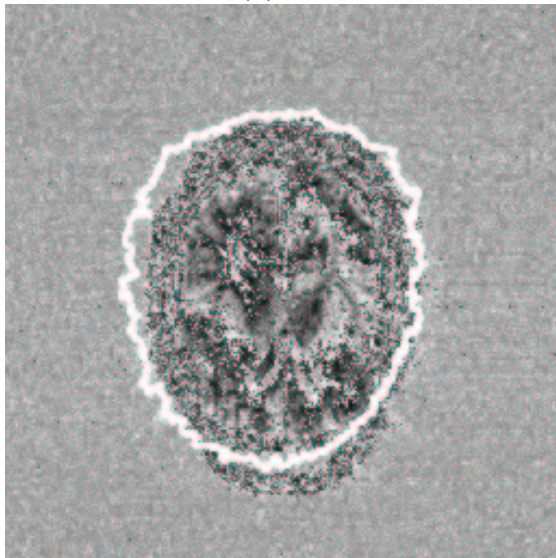


Figure 5.14: Column 1 and 2 are the results for registering reference point sets with small and large deformation respectively. (a)-(d) are the plots of the consistency error, measured by $\| T_{12} * T_{21} - I \|_F$ for the input transformation pair and $\| T_{12}^* * T_{21}^* - I \|_F$ for the GTLS output. While (c) and (d) are plots under different S.D of gaussian noise, (e) and (f) are plots for different proportion of outliers added.



(a): I_1

(b): I_2



(c): I_2 's boundary on I_1

(d): I_1 's boundary on I_2

Figure 5.15: Registering pair I_1 and I_2 .

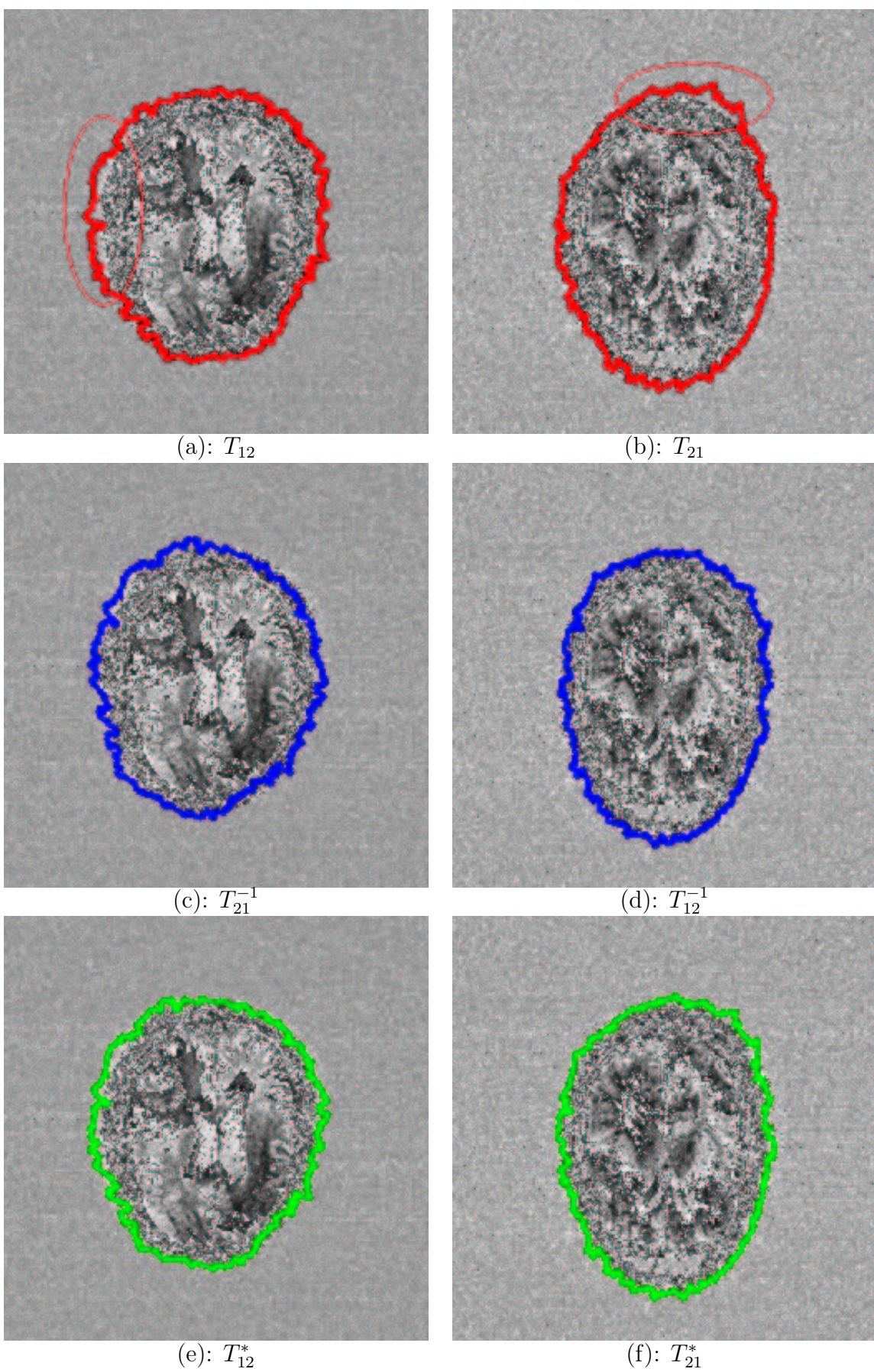


Figure 5.16: Registration results for the forward and backward registration process are shown in column 1 and column 2 respectively.

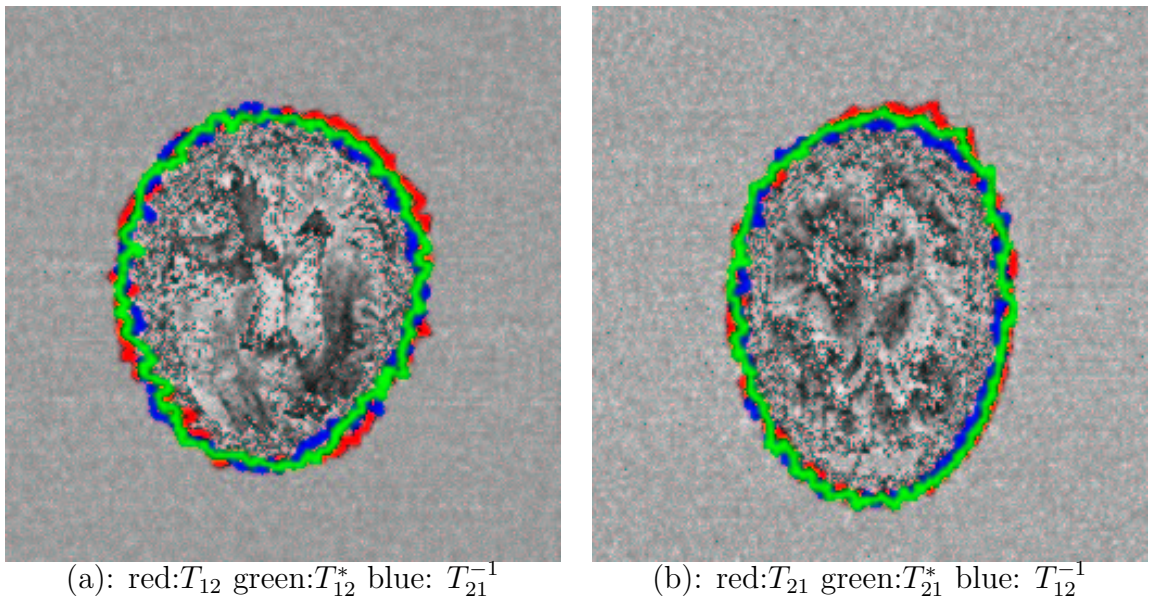


Figure 5.17: The registration results for the forward and backward registration process are shown in (a) and (b) respectively.

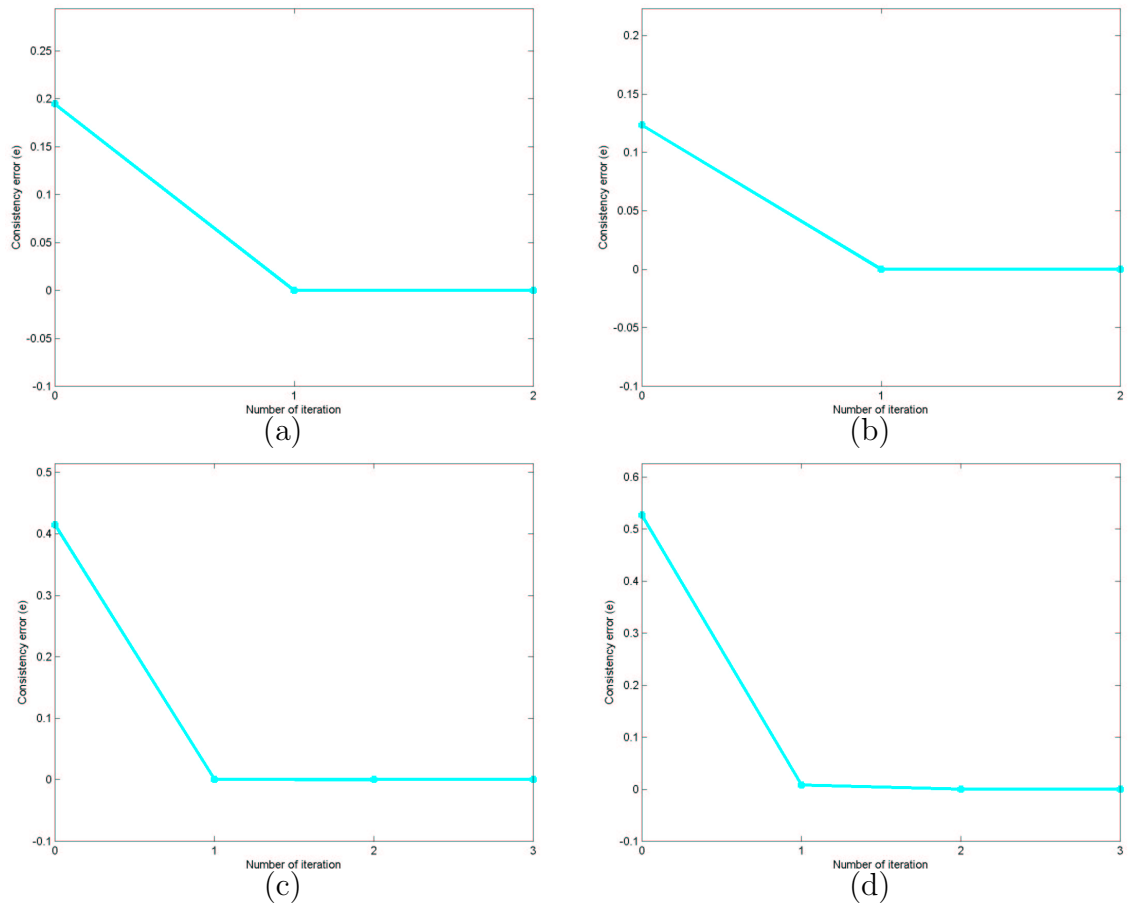


Figure 5.18: Convergence Profile (CP) example for experiments of brain point sets: (a): Small deformation + noise. (b): Large deformation + noise. (c): Small deformation + outliers. (d): Large deformation + outliers. The noise in (a) and (b) is gaussian noise with zero mean, S.D = 4. Outlier proportion = 0.4 in (c) and (d).

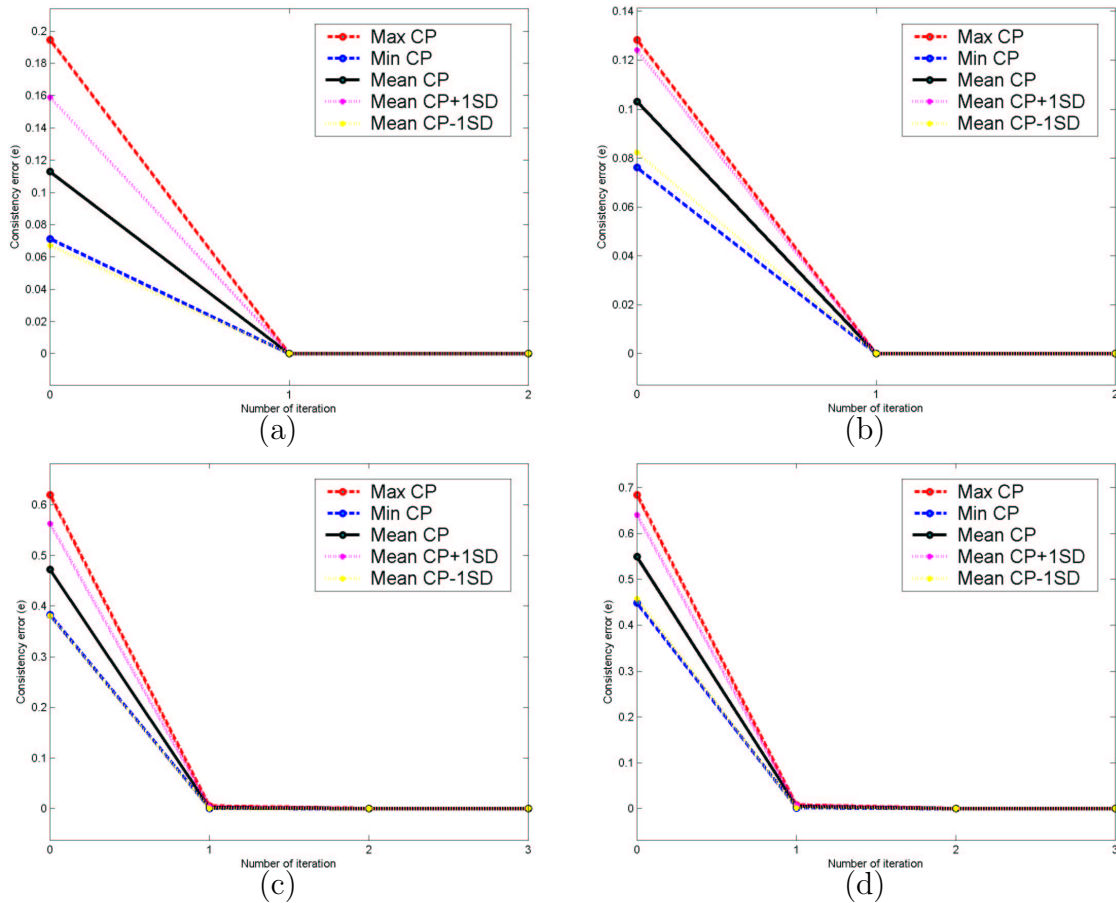
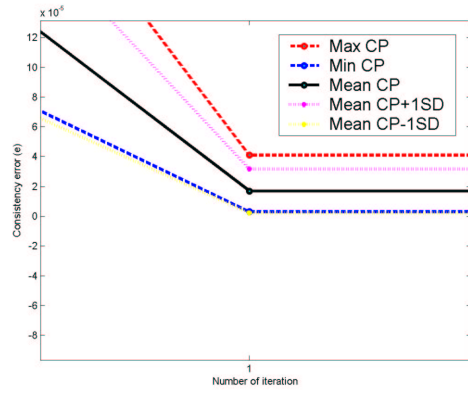
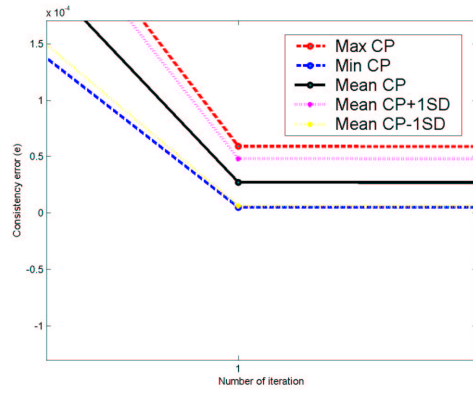


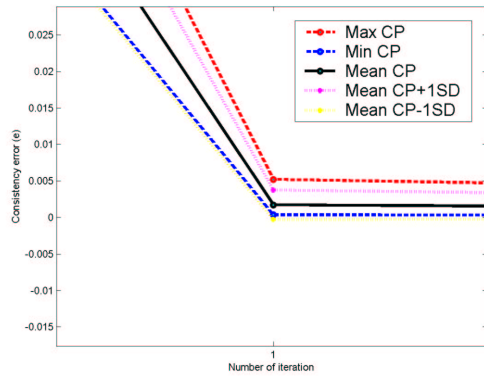
Figure 5.19: The mean value (Mean CP), together with the maximum value (Max CP), minimum value (Min CP) and ± 1 S.D. from the mean value (Mean CP+1SD/Mean CP-1SD) of the convergency profile from the studies of different amounts of noise or outliers. (a): Small deformation + noise. (b): Large deformation + noise. (c): Small deformation + outliers. (d): Large deformation + outliers. The number of studies in each case is 5.



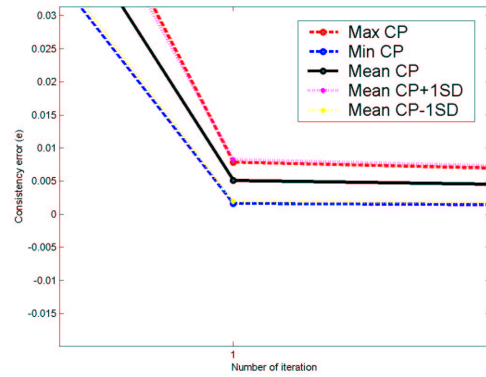
(a)



(b)



(c)



(d)

Figure 5.20: Zoom in of Fig.5.19

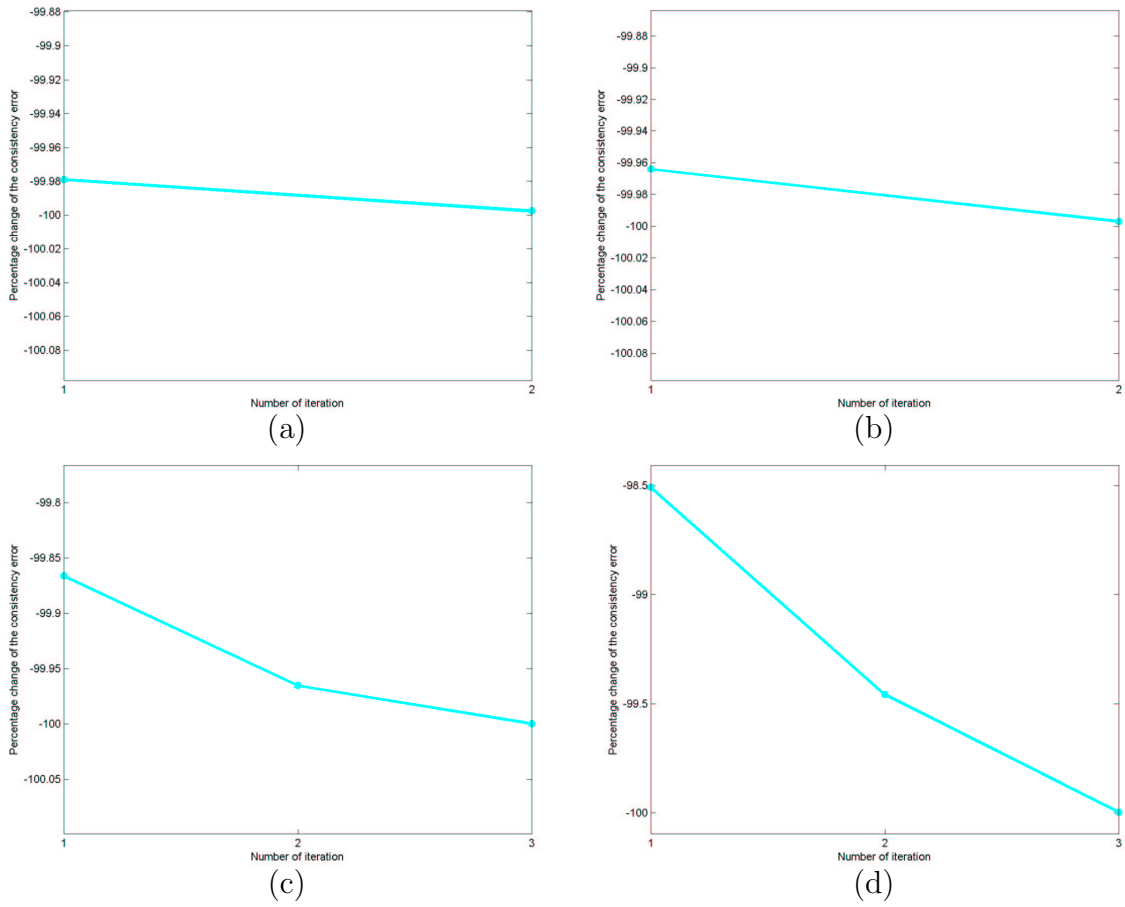


Figure 5.21: Percentage change of the convergence error shown in the convergence profiles in Fig.5.18. (a): Small deformation + noise. (b): Large deformation + noise. (c): Small deformation + outliers. (d): Large deformation + outliers.

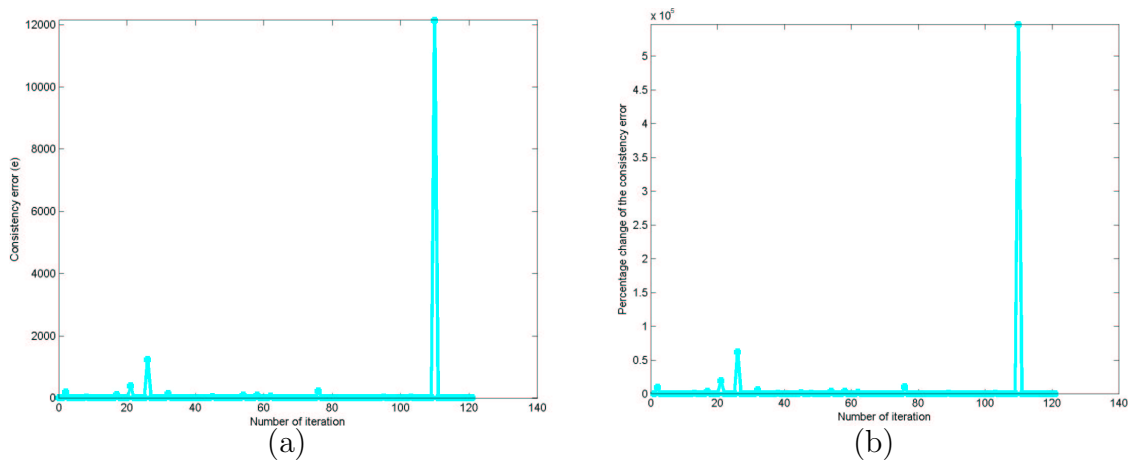


Figure 5.22: (a): An example of convergence profile which can not converge monotonically. (b): The percentage change of the convergence profile.



Figure 5.23: Input to the GTLS system which cause the problematic convergency in Fig.5.22. (a): The purple triangles are transformed from the blue circles by transformation matrix T_{12} . (b): The purple triangles are transformed from the blue circles by transformation matrix T_{21} . T_{12} and T_{21} is the transformation matrices pair for our system input.

Chapter 6

Conclusion

6.1 Summary

We presented a new framework for modelling the inverse consistency in registration, by simultaneously considering the stochastic uncertainties on both the transformation matrices and the inverse consistent constraint through the Generalized Total Least Square fitting from the transformation matrices obtained after the registration process. Our approach can be adopted to medical image registration problem [35] or general registration problem [36].

With our stochastic inverse consistent model, the uncertainty inherited from the discrete nature of the information sources is considered. Such uncertainty is illustrated in the wrong global maximum in the matching criteria such that the registration results obtained from conventional registration algorithms cannot achieve the real ground truth. The enforcement of the stochastic property on these forward and backward transformation matrices provides a mean apart from the matching criteria to achieve registration results which are closer to the ground truth.

Due to the underlying error within the forward and backward transformation matrices, deterministic imposition of the inverse consistent constraint from these erratic matrices will not help to improve the registration results in systematic way. Through our stochastic inverse consistency, the source-destination symmetric property will be enforced in a more systematic and flexible way such that the perfect inverse consis-

tency will be obtained when the uncertainty in the transformation is already minimized. In addition, our stochastic model can be imposed with the consideration of any other similarity constraints without compromising the weighting between the similarity measures and the inverse consistent constraint, it is theoretically more sensible than the incorporation of sub-objective cost function.

6.2 Future Work

In this thesis we are aiming at providing a new framework for modelling the inverse consistency in a post-registration fashion. In the future, we will examine whether it is better to incorporate the total least square fitting during the whole registration process. The affine transformation fitting will be extended to piecewise-affine or non-rigid deformation fitting to observe the possible improvement of the registration results in high dimensional deformation through inverse consistency.

The stochastic property of the individual element of the forward and backward transformation matrices, their relationship within the matrix and also the interrelation among a pair of transformation matrices will be examined extensively. The relationship of the inverse consistent model with input forward and backward transformation matrices and the stochastic property representing the imperfectness of the inverse consistent constraint will also be studied in the future work. All of these are potential means to establish better registration results through inverse consistency.

Bibliography

- [1] BrainWeb: (Mcgill) <http://www.bic.mni.mcgill.ca/brainweb/>.
- [2] R. Bajcsy and S. Kovacic. Multiresolution elastic matching. *Comput. Vision Graph. Image Process.*, 46(1):1–21, 1989.
- [3] Paul J. Besl and Neil D. McKay. A method for registration of 3-d shapes. *IEEE Trans. Pattern Anal. Mach. Intell.*, 14(2):239–256, 1992.
- [4] Fred L. Bookstein. Principal warps: Thin-plate splines and the decomposition of deformations. *IEEE Trans. Pattern Anal. Mach. Intell.*, 11(6):567–585, 1989.
- [5] Max Born and Emil Wolf. *Principles of optics : electromagnetic theory of propagation, interference and diffraction of light*. Cambridge University Press.
- [6] John Canny. A computational approach to edge detection. *IEEE Trans. Pattern Anal. Mach. Intell.*, 8(6):679–697, 1986.
- [7] Gary E. Christensen. Consistent linear-elastic transformations for image matching. In *IPMI*, pages 224–237, 1999.
- [8] Gary E. Christensen. Inverse consistent registration with object boundary constraints. In *ISBI*, pages 591–594, 2004.
- [9] Gary E. Christensen and Hans J. Johnson. Consistent image registration. *IEEE Trans. Med. Imaging*, 20(7):568–582, 2001.
- [10] Gary E. Christensen, Richard D. Rabbitt, and Michael I. Miller. Deformable templates using large deformation kinematics. *IEEE Trans. Image Processing*, 5(10):1435–1447, October 1996.

- [11] Haili Chui and Anand Rangarajan. A new algorithm for non-rigid point matching. In *CVPR*, pages 2044–2051, 2000.
- [12] James S. Duncan and Nicholas Ayache. Medical image analysis: Progress over two decades and the challenges ahead. *IEEE Trans. Pattern Anal. Mach. Intell.*, 22(1):85–106, 2000.
- [13] Raúl San José Estépar, Anders Brun, and Carl-Fredrik Westin. Robust generalized total least squares iterative closest point registration. In *MICCAI (1)*, pages 234–241, 2004.
- [14] Hongyu Guo, Anand Rangarajan, S. Joshi, and Laurent Younes. Non-rigid registration of shapes via diffeomorphic point matching. In *ISBI*, pages 924–927, 2004.
- [15] Jianchun He and Gary E. Christensen. Large deformation inverse consistent elastic image registration. In *IPMI*, pages 438–449, 2003.
- [16] Hans J. Johnson and Gary E. Christensen. Consistent landmark and intensity-based image registration. *IEEE Trans. Med. Imaging*, 21(5):450–461, 2002.
- [17] Kiriakos N. Kutulakos and Steven M. Seitz. A theory of shape by space carving. *International Journal of Computer Vision*, 38(3):199–218, 2000.
- [18] Frederik Maes, André Collignon, Dirk Vandermeulen, Guy Marchal, and Paul Suetens. Multimodality image registration by maximization of mutual information. *IEEE Trans. Med. Imaging*, 16(2):187–198, 1997.
- [19] J.B.A. Maintz and M.A. Viergever. A survey of medical image registration. *Medical Image Analysis*, 2(1):1–36, April 1998.
- [20] Chen G. T. Y. Spelbring D. R. Weichselbaum R. R. Pelizzari, C. A. and C. T. Chen. Accurate three-dimensional registration of ct, pet, and/or mr images of the brain. *J. Comput. Assist. Tomogr*, 13(1):20–26, 1989.

- [21] Anand Rangarajan, Eric Mjolsness, Suguna Pappu, Lila Davachi, Patricia S. Goldman-Rakic, and James S. Duncan. A robust point matching algorithm for autoradiograph alignment. In *VBC*, pages 277–286, 1996.
- [22] Karl Rohr, H. Siegfried Stiehl, Rainer Sprengel, Thorsten M. Buzug, Jürgen Weese, and M. H. Kuhn. Landmark-based elastic registration using approximating thin-plate splines. *IEEE Trans. Med. Imaging*, 20(6):526–534, 2001.
- [23] Oskar M. Skrinjar and Hemant Tagare. Symmetric, transitive, geometric deformation and intensity variation invariant nonrigid image registration. In *ISBI*, pages 920–923, 2004.
- [24] Colin Studholme, Derek L. G. Hill, and David J. Hawkes. An overlap invariant entropy measure of 3d medical image alignment. *Pattern Recognition*, 32(1):71–86, 1999.
- [25] G. Subsol. Crest lines for curve based warping. *Brain Warping*, pages 225–246, 1998.
- [26] J.-P. Thirion. Image matching as a diffusion process: an analogy with maxwell’s demons. *Medical Image Analysis*, 2(3):243–260, 1998.
- [27] P. M. Thompson and A. W. Toga. A surface-based technique for warping three-dimensional images of the brain. *IEEE Trans. Med. Imaging*, 15(1):1–16, Aug. 1996.
- [28] Carole J. Twining and Stephen Marsland. Constructing diffeomorphic representations of non-rigid registrations of medical images. In *IPMI*, pages 413–425, 2003.
- [29] P. A. van den Elsen, E. J. D. Pol, and M. A. Viergever. Medical image matching—a review with classification. *IEEE Engineering in Medicine and Biology Magazine*, 12(1):26–39, March 1993.

- [30] S. Van Huffel and J. Vandewalle. Analysis and properties of the generalized total least squares problem $AX \approx B$ when some or all columns in A are subject to error. *SIAM J. Matrix. Anal. Appl.*, 10:294–315, 1989.
- [31] S. Van Huffel and J. Vandewalle. *The Total Least Squares Problem: Computational Aspects and Analysis*, volume 9 of *Frontiers in Applied Mathematics*. SIAM, Philadelphia, 1991.
- [32] Paul Viola and William M. Wells, III. Alignment by maximization of mutual information. *International Journal of Computer Vision*, 24(2):137–154, 1997.
- [33] J. West, J. M. Fitzpatrick, et al. Comparison and evaluation of retrospective intermodality brain image registration techniques. *Journal of Computer Assisted Tomography*, 21(4):554–566, 1997.
- [34] George Wolberg. Recent advances in image morphing. In *Computer Graphics International*, pages 64–, 1996.
- [35] Sai Kit Yeung and Pengcheng Shi. Stochastic inverse consistency in medical image registration. In *MICCAI*, 2005.
- [36] Sai Kit Yeung and Pengcheng Shi. Stochastic inverse consistent registration. In *EMBC*, 2005.
- [37] Young T. Y. Zhao, W. and M. D. Ginsberg. Registration and three-dimensional reconstruction of autoradiographic images by the disparity analysis method. *IEEE Trans. Med. Imaging*, 12(4):782–791, 1993.